Journal of Earth Sciences and Geotechnical Engineering, Vol. 10, No. 5, 2020, 87-130
ISSN: 1792-9040 (print version), 1792-9660 (online)
Scientific Press International Limited

Possibilities and Limitations in Using Smectite Clay for Isolating High-Level Radioactive Waste (HLW)

Roland Pusch[1], Richard Weston[2] and Jörn Kasbohm[3]

Abstract

Global interim storage of HLW has reached a level that requires large extension of the storage capacity, which puts pressure on regulatory authorities and national parliaments for finding and applying ways of safe disposal of such waste. An important option is to use very dense natural expandable clay for isolating spent nuclear fuel in boreholes where it will be exposed to high temperature for hundreds to a few thousand years. The clay must be placeable and homogeneous and be able to sustain significant shear strain and temperatures up to 150^{o}C without leaking or losing its ductile behaviour and self-healing potential. In this document the long-term function of such seals, which have the form of dense smectite blocks and soft smectite mud surrounding the containers/canisters will be described with respect to the impact of degrading physical/chemical mechanisms. Focus is on clay barriers for isolating spent nuclear fuel in up to 3-4 km deep boreholes but aspects are also provided on disposal in mined repositories at a few hundred m depth below the ground surface.

In either case the dense clay surrounding the waste containers will expand and enclose them, and consolidate the surrounding mud, which successively becomes denser, while the dense clay seal softens until its swelling pressure and the pressure of the mud is the same.

The clay seals in deep boreholes used for disposal of spent nuclear fuel consist of a central core of dense expandable clay in perforated tubes ("supercontainers") submerged in clay mud according to a concept termed VDH. In the lower parts of 3-4 km deep boreholes these tubes, made of copper, Navy Bronze, titanium or steel, host canisters lined with highly compacted expandable clay. In the upper parts of the holes the same type of supercontainers with no waste but with dense smectite

[1]Department of Civil, Environmental and Natural Resources Engineering, Luleå University of Technology, Sweden,
[2]Department of Production and Materials Engineering, Lund University, Sweden.
[3]Geoencon and Greifswald University (Miner. Dep.), Germany

Article Info: *Received:* July 10, 2020. *Revised:* July 27, 2020.
Published online: August 2, 2020.

clay blocks make up a primary barrier to possibly released radionuclides. A second barrier is the heaviness of the strongly saline groundwater at depth, which prevents such water to reach high up to the biosphere. The role of the mud is to save the supercontainers from touching the borehole walls when being placed, and to seal voids in the borehole walls with clay. The dense clay and soft clay mud will interact physically and ultimately become a homogeneous silicified clay body. Creep strain in the rock causes the deposition holes to con, which increases the radial pressure on the clay seals and thereby eliminates flow and diffusive migration of possibly contaminated porewater from the deployment part to move to the ground surface.

Keywords: Smectite, High Level Radiation Waste (HLW), VDH Concept, Clay.

1. Scope of study

The paper focuses on clay seals in boreholes for disposal of spent HLW, placed to avoid intersection by water-bearing fracture zones. Several versions of this and similar concepts have been described and examined in the literature and much effort has been paid to describe the function in short perspectives but with limited attention to the long-term ability to effectively isolate such waste. This matter is discussed here focusing on the longevity of the clay seals.

2. Introduction

The VDH seals consist of perforated tubes of copper, Navy Bronze, titanium or steel, filled with fresh-water saturated, very dense expandable clay (smectite). They are placed by drill rigs in large-diameter boreholes from the ground surface or from shallow tunnels with the holes filled with soft to medium-dense smectitic mud in which the tubes are left at intended levels so that the clay can expand through the perforations for sealing off the holes. The dense clay and soft mud will interact physically and ultimately make up homogeneous and impermeable clay seals. In the lower part of 3-4 km deep boreholes the tubes host HLW canisters of the same metal containing HLW in the form of spent reactor fuel. In the upper parts of the holes the containers hold only dense smectite clay blocks. In the upper parts central dense cylindric clay blocks occupy the supercontainers that are placed by moving them down in soft mud of expandable clay. The role of the mud is to save the supercontainers from touching the borehole walls when placed, and to seal voids and fractures by clay in the borehole walls. The dense clay and soft clay mud will interact physically and ultimately become a homogeneous clay seal. Once the supercontainers have reached the intended positions the clay and mud will physically mature which can take several years for big seals. In parallel, the mineral composition and physical properties will slowly change by chemical impact. This will lead to strengthening, stiffening and alteration of the stress/strain properties of the clay seal components and will thereby affect the ability to preserve the waste-isolating potential of the clay seals. If the holes are located in argillaceous rock, the creep potential will converge the holes and eliminate the risk of axially leaching

radioactively contaminated water.

3. Fundamental physical behaviour of clay for isolation of HLW

3.1 The KBS-3V concept, preparation of clay seals

The raw material is crushed and sieved to get a suitable grain size distribution, which implies 100 % granules smaller than 10mm, 90% smaller than 1mm, 80% smaller than 0.5mm, 20% smaller than 0.08mm and 0% smaller than 0.01mm. Such materials can be used to compact blocks with about 10% water content and a dry density of 100 to 2000kg/m^3 (Figure 1). Once the maturation process is complete underground, the physical function of the clay seal can be defined by use of soil mechanical principles (cf. Pusch et al, 2011).

Figure 1: Placement of a 2000kg clay block with 1.80m diameter of smectite-rich clay (MX-80) being placed in a shallow deposition hole in SKB's ÅSPÖ underground laboratory (Photo: Ramqvist).

3.2 The VDH concept

The most essential properties of clays used for isolation of HLW is low hydraulic conductivity and high expandability and self-healing ability. The clay must be placeable and homogeneous and be able to sustain large shear strain without leaching radionuclides. Deposition is made in holes with 0.50 to 0.80m diameter bored to a depth of 3-5km depth in crystalline or argillaceous rock.

The supercontainers, which can be made of copper, Navy Bronz, titanium or steel, are placed in holes that are filled with soft to medium dense smectitic mud throughout all the field work, including boring of the holes, placement of the containers, casting of concrete where water-bearing fracture zones are intersected, and final plugging of the upper ends of the holes with talc-based concrete (Pusch et

al, 2018).

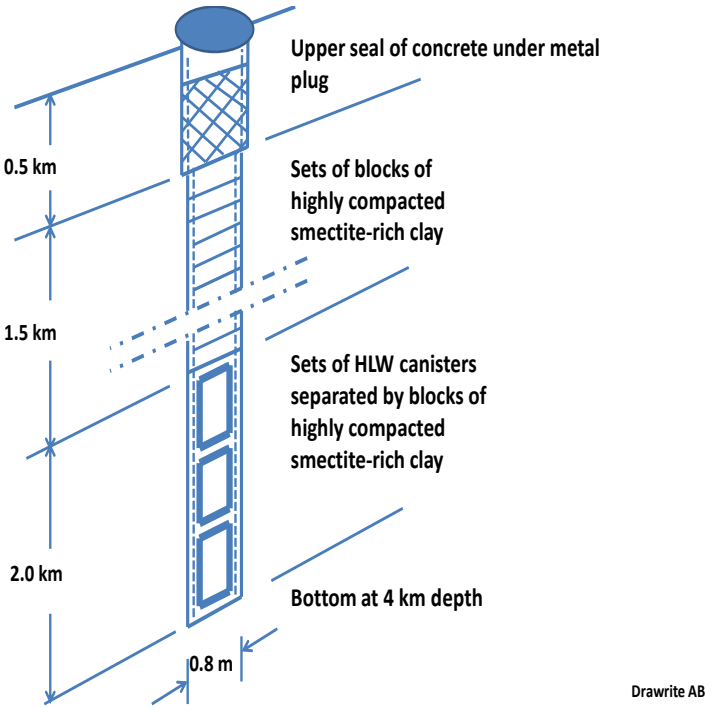

Figure 2: Schematic view of VDH with constant diameter below the uppermost seal of concrete that extends to 0.5km depth, below which the hole contains clay seals to 2km depth. The lowest "deployment" zone with HLW canisters separated by clay blocks is shown here in a hole with 0.8m diameter. Where the holes pass through wet fracture zones concrete is cast on site.

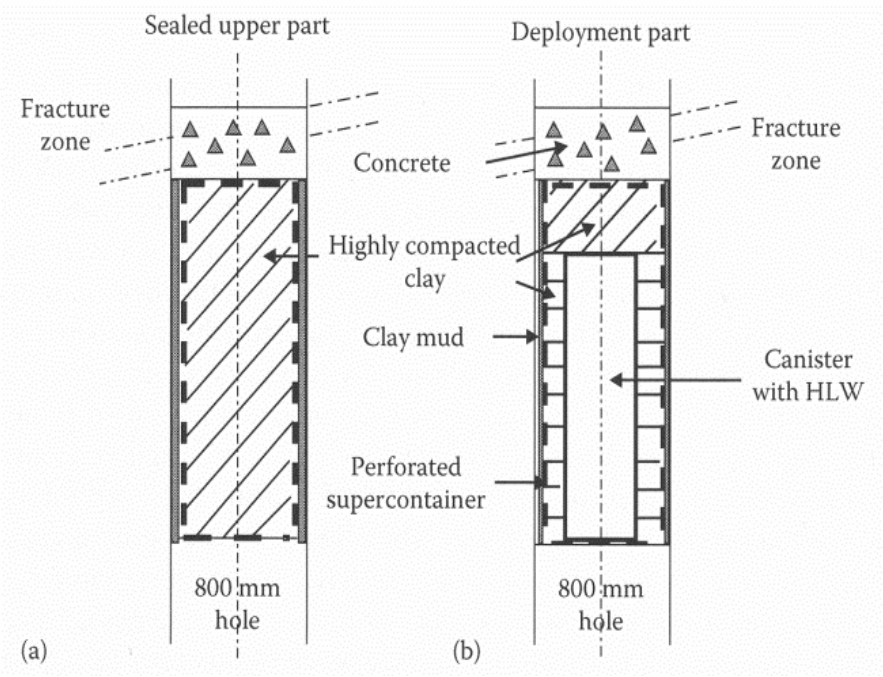

Figure 3: "Supercontainers" in VDH, a) From 0.5 to 1.5km depth they are filled with blocks of highly compacted clay. b) From 2-4km depth they contain HLW canisters surrounded by highly compacted clay.

The supercontainers with waste canisters of the same material, and with clay provide a primary engineered barrier to migration of possibly released radionuclides from the lower parts of the holes while the heaviness of the salt groundwater in the deployment zone serves as a second isolation of the waste. The lack of significant hydraulic gradients means that there are no driving forces for bringing radioactively contaminated water up to the biosphere; the only transport mechanism is diffusion of dissolved radionuclides but the very long transport paths rule out this risk.
Three conditions in the matured clay combine to provide extra safe conditions for long-term isolation of highly radioactive waste:

i. homogeneity and low hydraulic conductivity.
ii. ability to self-heal after thermally or seismically generated shear strain without causing pathways for leaching radionuclides.
iii. preservation of ductile behaviour.

The first item implies that the ultimate dry density (ρ_d) of the clay seal is higher than about 1,900kg/m^3 and lower than 2,200kg/m^3. The maximum value is set for avoiding swelling pressure that can damage the waste containers. The intended density gives the clay a hydraulic conductivity K of E-14 to E-11m/s, which is required by IAEA and several national authorities (Pusch et al, 2018). The

homogeneity must be certified, implying that the dry density should not vary by more than +/- 100kg/m^3 from the mean value of test samples.
The second item means that the expandability must be sufficient to avoid creation and preservation of local erosive leakage of radioactively contaminated groundwater
The third item implies that the chemical conditions in the clay seals do not cause brittleness and associated loss of the self-healing potential of the clay seals.

3.3 Clay candidates-Bentonites

Smectite-rich natural clay like bentonite is recommended for use as effective seals, cf. Table 1.

Table 1: Examples of main geotechnical data of commercially available smectitic clay candidates for isolating highly radioactive waste. K=Hydraulic conductivity in m/s; ps,= Swelling pressure in MPa. The data refer to saturation/percolation with low-electrolyte water ("A") and 3.5 % CaCl2 solution ("B"); data are given as (A)/(B). C=Weight % of expandable minerals (Pusch, 2018). (cf. Figure 4).

Dry density [kg/m^3]	C [%]	K [m/s]	p_s [MPa]	Undrained shear strength [kPa]
1750	70-90	(E-14)/(5E-13)	12.0/12.0	2000
1590	70-90	(5E-13)/(E-13)	6.0/6.0	1800
1430	70-90	(E-13)/(5E-13)	1.0/1.0	1000
1270	50-70	(5E-13)/(E-12)	0.9/0.8	800
1110	40-60	(E-12)/(5E-12)	0.2/0.1	600
950	20-40	(5E-12)/(E-11)	0.1/0	400
790	0.5-10	(5E-11)/(E-10)	0.1/0	200-500

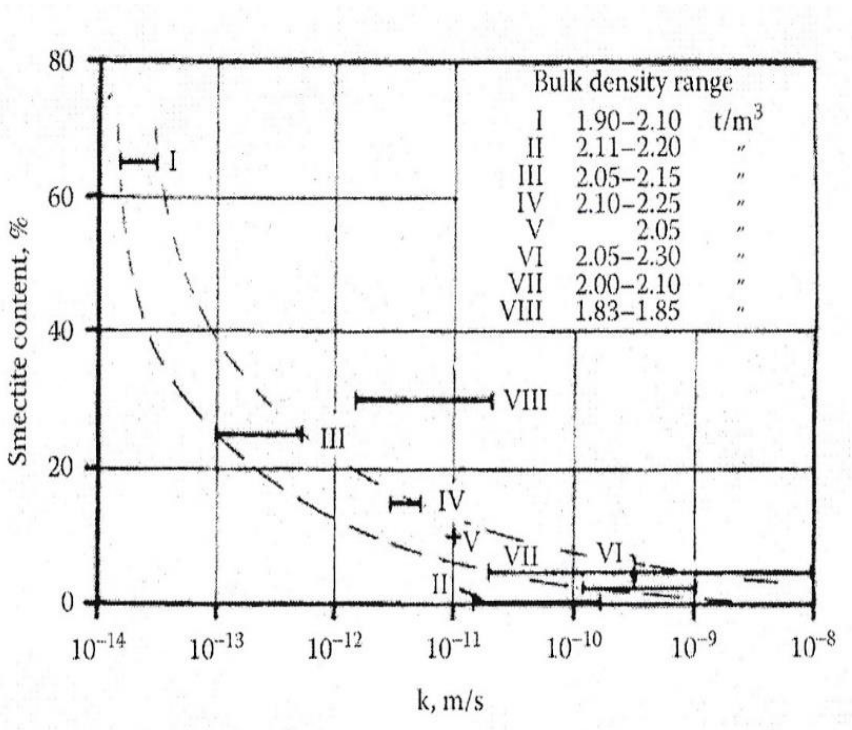

Figure 4: Hydraulic conductivity (k) as a function of the smectite content of smectitic clays. I is Cretaceous clay with 60-70% smectite, II is Silurian clay with less than 5% smectite, III is Ordovician clay with 20-30% smectite, IV is Ordovician clay with 15-25% smectite, V is Belgian Boom mixed-layer clay with 10-15% smectite, VI is clay-weathered crystalline rock with 2-10% smectite, and VII and VIII are Cretaceous bentonites. The anomalous behaviour of the Danish Fish clay (VIII) is explained by its low bulk density in water saturated form. Data from Pusch and Yong, 2006.

The very low hydraulic conductivity and the strong expandability of smectitic clays make them superior to non-smectite ones. However, with time smectites become converted to non-expandable clay the function of which hence determines the long-term waste isolation capacity.

The required self-healing ability is related to the swelling pressure and creep potential of expandable clays. This pressure is of osmotic nature and is largely dependent on the amount of hydrate layers in the smectite particles which consist of 10Å lamellae separated by viscous "interlamellar water" according to Table 2.

The coordination of inter- and extra-lamellar water molecules and cations and the crystal lattice atoms depends on the size and charge of the cations and on the charge distribution in the lattice. Three hydrate layers implying complete water uptake can only be formed in some of the smectite species, and normally only when sodium, lithium or magnesium are in interlamellar positions (Table 2). One finds from this table that montmorillonite is the only smectite mineral of the listed ones that can

expand to form 3 interlamellar hydrates. Illite, being a reaction product of hydrothermally affected smectite, is less expandable than smectite in the nature or in a repository.

Table 2: Number and thickness of interlamellar hydrates in nm (After Kehres).

Smectite clay type	M[1)]	1st hydrate	2nd hydrate	3rd hydrate
Montmorillonite	Mg	0.30	0.30	0.30
	Ca	0.39	0.28	-
	Na	0.30	0.32	0.35
	K	0.24	0.37	-
Beidellite	Mg	0.27	0.27	-
	Ca	0.23	0.23	-
	Na	0.22	0.22	-
	K	0.25	-	-
Nontronite	Mg	0.29	0.30	-
	Ca	0.31	0.34	-
	Na	0.27	0.28	-
	K	0.26	-	-

We will consider borehole seals of smectitic clay and focus on the homogenization of the two smectite clay components shown in Figure 5, which represents a key issue for HLW disposal. The clay mud and dense clay of compacted smectite clay are confined in a perforated metallic supercontainer with or without HLW, and placed in soft smectite mud.

The VDH concept implies that the deep holes with HLW in their lower parts are sealed off by dense smectitic clay and intermittently by concrete where the holes intersect water-bearing fracture zones. Figure 5 shows the design principle of clay seals with a very dense, expansive core of smectite-rich clay prepared by saturation with low-saline water. Maturation of the clay seal involves expansion of the central clay core causing consolidation of the mud under the swelling pressure exerted by the clay core. The process includes microstructural changes and motion of porewater and clay particles to reach a stable state. The matured clay seal will expand until the swelling pressure at the contact with the confining rock is fully developed. Long-term modelling of the expansion or shrinkage caused by changes in effective stress by loading/unloading or by change in groundwater chemistry has to be predicted in the design.

Integration of the initially heterogeneous seal of smectite clay and the surrounding smectitic mud evolves to form homogeneous embedment of the perforated tube as seen in Figure 6.

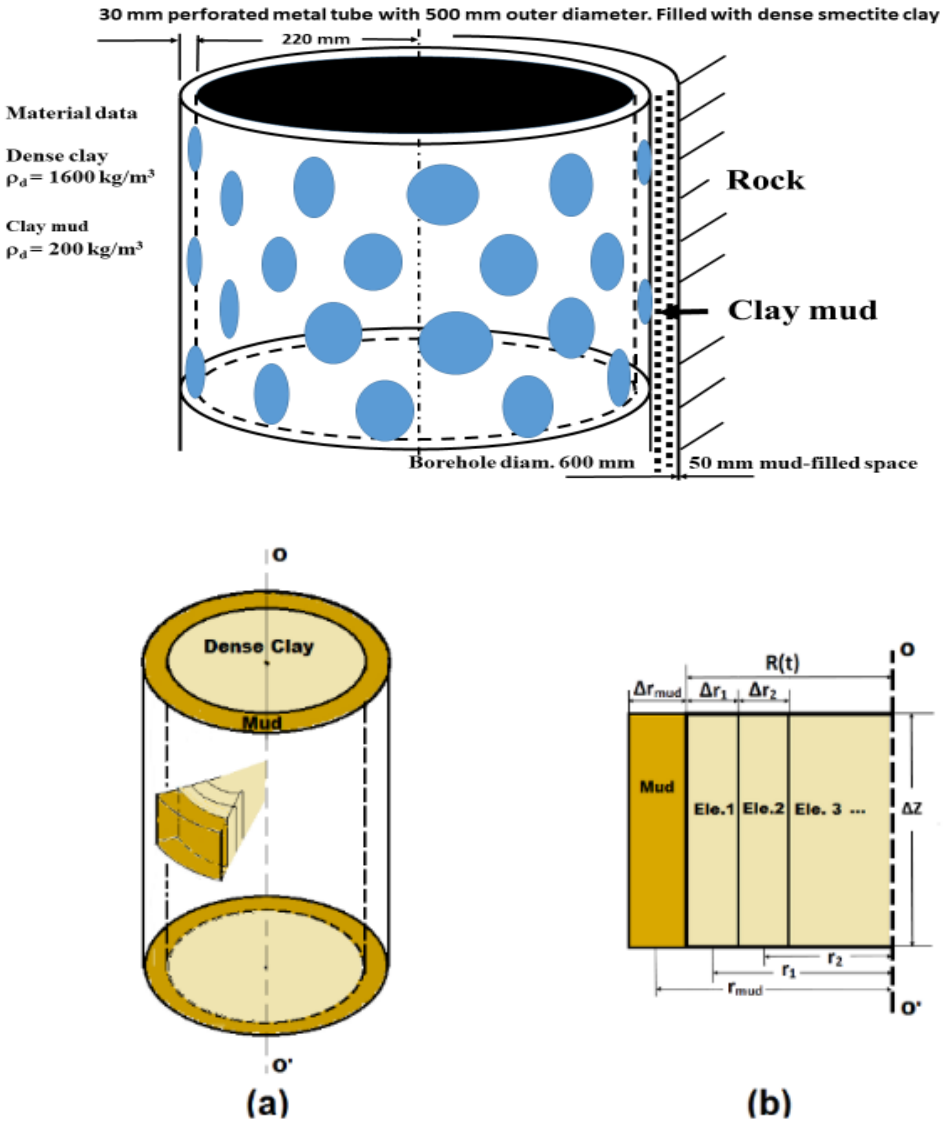

Figure 5: Example of VDH clay seal in a borehole.
Upper: Perforated supercontainer with dense clay core submerged in medium-soft smectite mud. Lower: Annular elements for calculating maturation (Yang et al, 2015).

Figure 6: Maturation[4] of clay seal. Left: Clay expanded radially through the perforated tube by adsorbing low-electrolyte water for 8 hours. Right: 24 hour old seal of dense clay in smectite clay mud with an initial dry density of 200kg/m^3.

3.4 Preparation and maturation of clay seals

The raw material is crushed and sieved to get a suitable grain size distribution, which implies 100% granules smaller than 10mm, 90% smaller than 1mm, 80% smaller than 0.5mm, 20% smaller than 0.08mm and 0% smaller than 0.01mm. Such materials can be used to compact blocks with about 10% water content and a dry density of 100 to 2000kg/m^3 (Figure 4). Maturation of a clay seal involves porewater migration and transport of clay particles from the dense clay core to the clay mud as indicated in Figure 6. The radial transport of water from the mud to the dense, water saturated clay core in the maturation phase follows Darcy's law for complete saturation of the clay, which is guaranteed by the large depth of the boreholes. Once the maturation process is complete the physical function of the clay seal can be defined by use of soil mechanical principles (cf. Pusch and Yong, 2006). The following conditions, corresponding to those in a real VDH with initially fully water saturated mud and dense clay, are assumed:

- The supercontainers with HLW canisters and dense clay are located in pervious rock, i.e. the boring-disturbed zone with enhanced hydraulic conductivity (EDZ), represented by a water saturated sand filter in model tests (Yang et al, 2015). Either case provides water to be absorbed or expelled from the clay seal.
- The supercontainers are forced down in the mud to rest on already placed ones.

- The total volume of dense clay and mud is constant during the entire maturation process.
- Migration of water and solids in the maturation process take place only in radial direction.
- Maturation, which involves redistribution of porewater and associated microstructural changes including dispersion of clay, takes place under isothermal conditions.

In practice and in modelling, minor local hydraulic gradients are generated by differences in hydration potential between adjacent clay elements with different dry densities and water content (Figure 7). The high hydration potential of the central dense clay core brings water in the mud to move into the dense clay, which will thence contain more water and undergo a drop in density and thereby a reduction of the hydration potential.

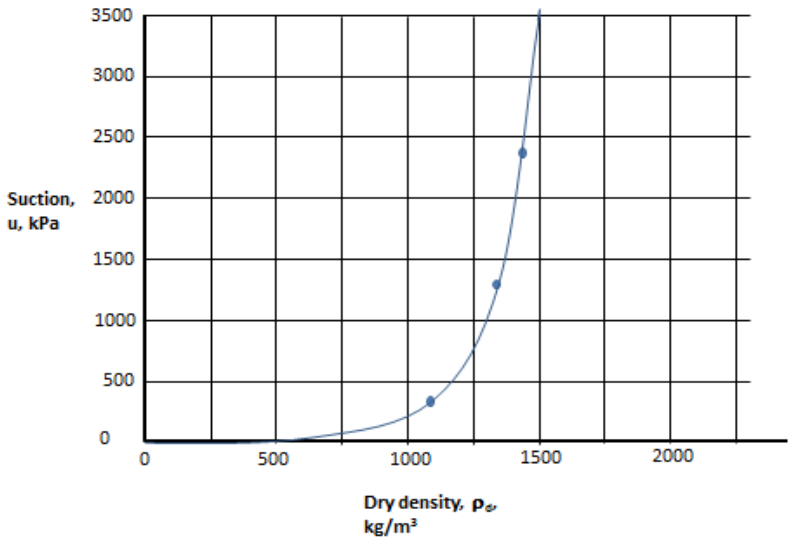

Figure 7: Example of the suction potential of water saturated montmorillonite-rich clay.

Clay particles will be exfoliated from the dense clay as exemplified by Figure 8 and migrate into the mud through the perforation of the confining tube. By this, all the annular elements in Figure 5 will successively become less dense, while all mud elements will become denser. The hydration/dehydration process depends on the position of the clay elements and on time. The elements are subject to consolidation or swelling, implying only radial water flow and migration of clay particles.

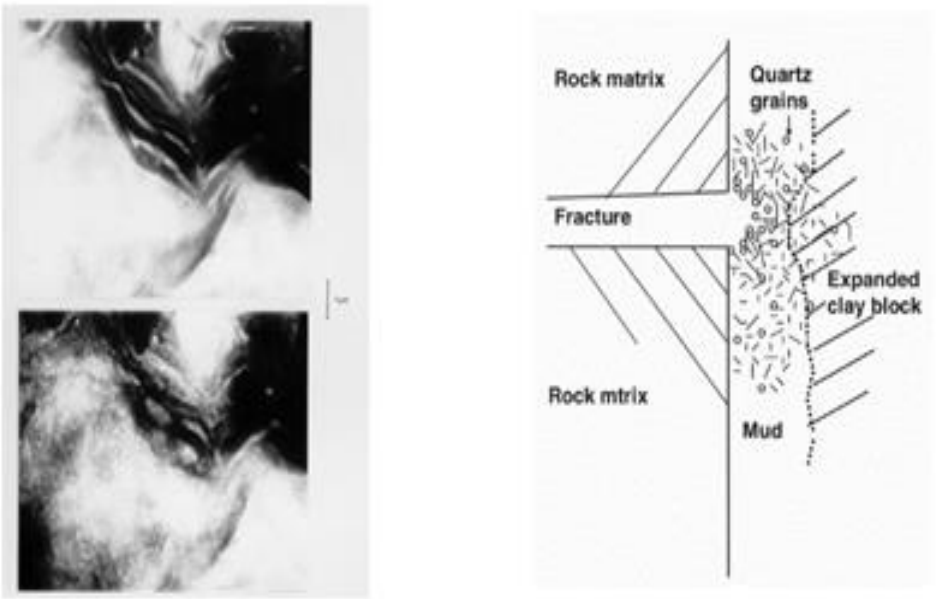

Figure 8: Smectite seal. Left: swelling of dried montmorillonite specimen in CNRS' high-voltage transmission electron microscope on wetting. Right: Expansion of clay mud into rock fracture. The content of quartz particles causes arching and stop of loss of clay.

A theoretical model of the maturation of composite clay seals in boreholes has been formulated and experimentally verified by Yang et al (2015) by use of a corresponding physical model consisting of a dense core of smectite-rich clay submerged in smectitic clay mud, the system being confined in a 100mm diameter perforated tube. The water content and dry density of the clay within and adjacent to the perforated tubes were determined after 24 hours and 14 days, respectively. The central dense clay core had an initial dry density of 1,650kg/m3 while the mud had an initial dry density of 120kg/m3. Basic raw material data of the clay used in various tests are collected in Table 3 and data from parallel physical model tests are shown in Table 4.

Table 3: Raw material data for natural Holmehus clay used in the model test (Yang, 2015).

Dry density, [kg/m^3]	Water content [weight percent]	Plastic limit [%]	Liquid limit [%]	Clay content (<2 μm) [%]	Montmorillonite content of clay fraction [%]
1,630-1,650	10-15	30-35	220-230	50-60	50-60

Table 4: Model test data of clay outside the perforated tube that was initially clay mud with a dry density of 120kg/m^3 (cf. Figure 6). The initial average dry density ρ_d of the dense clay was 1,600kg/m^3 and w is water content in weight percent (Yang, 2015).

Part of clay seal (cf. Figure 5)	24-hour test		14-day test	
	w	ρ_d	w	ρ_d
1mm "skin" between "plugs"	305	320	65	950
"Plugs" moved out from tube	235	360	45	1190
Clay betw. protruding "plugs"	275	310	65	950

An important finding from such model tests is that the clay "skin" surrounding the perforated tube was uniform after 24 hours (cf. Figure 7), the dry density having increased from the average initial value 120kg/m^3 to 320kg/m^3, implying a hydraulic conductivity of about E-10m/s and a swelling pressure of a few tens of kPa. The dry density subsequently increased to about 950kg/m^3 giving a swelling pressure of several tens of kPa in two weeks, which, in practice, provides strong physical interaction with the supercontainer and the surrounding rock. The diagram in Figure 7 shows that almost one year was needed for homogenization of the model clay seal at which point the entire clay seal got an average dry density of about 1,200kg/m^3. This indicates that large-diameter clay seals will not be homogeneous until several years after placement in deposition holes with 0.5m or larger diameter. They will, however, be enough mature to resist percolation much earlier since hydraulic gradients will never drive porewater vertically through kilometers of VDH clay seals. Attempts to perform theoretical modelling of the maturation process that includes porewater and clay migration have been made and we will show the main steps in a successful project (Yang et al, 2015). The procedure is based on the physical model in Figures 3 and 4 involving radial migration of clay particles and water. Water flow into and out from each annular element to the adjacent ones during each time step takes place according to Darcy's law under the radial hydraulic gradient being the transient net suction potential of adjacent elements:

$$q = AKi \tag{1}$$

where q is the radial water flow per permeated cross area A of the clay seal, i being the hydraulic gradient, and K the hydraulic conductivity.

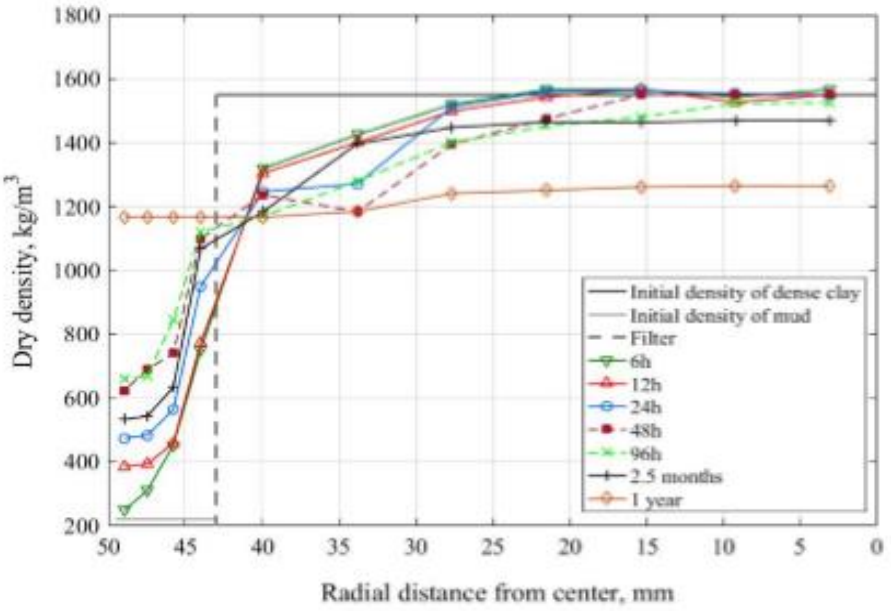

Figure 9: Evolution of model VDH clay seal showing successive densification of smectite mud (left part) and softening of dense montmorillonite-rich clay in the perforated supercontainer (cf. Figure 4). The broken line at 43mm distance from the center represents the outer diameter of the model container with the vertical symmetry axis at "0" (Yang, 2015).

Application of the described model implies stepwise computation repeated iteratively using constant time steps (Yang et al, 2015). For the total computation time T and the maturation time for each time step Δt, the time steps t are hence equal to $[\frac{T}{\Delta t}]$. Water migration in the constantly saturated clay elements (n), calculated by use of the values of hydraulic conductivity and the different suction potential of adjacent elements, implies water transport from the center of the composite clay unit $r_{(n-1)}(t)$ to the adjacent one $r_n(t)$. In this context it should be mentioned that other designs of expandable clay seals have been successfully tested like the one in Figure 10 with dense smectite granules dispersed in soft smectite clay mud. They also mature by the potential of dense smectite clay to expand and homogenize. Palygorskite is a fibrous smectite mineral that makes the mixture with montmorillonite strongly thixotropic.

**Figure 10: Borehole seal of smectite granules mixed into mud.
Left: Sectioned sample at start of water uptake.
Right: Largely homogeneous state after 40 days (Pusch et al, 2011).**

3.5 Degrading processes in matured clay seals

Two types of processes can negatively affect the performance of smectite clay seals and damage their waste-isolating capacity, i.e. the just described impact of shearing by seismicity/tectonics and creep, and chemical impact like cation exchange and hydrothermal effects causing cementation. Shearing of deep sealed boreholes can take place where the holes are intersected by continuous discontinuities like major fracture zones (Figure 11).

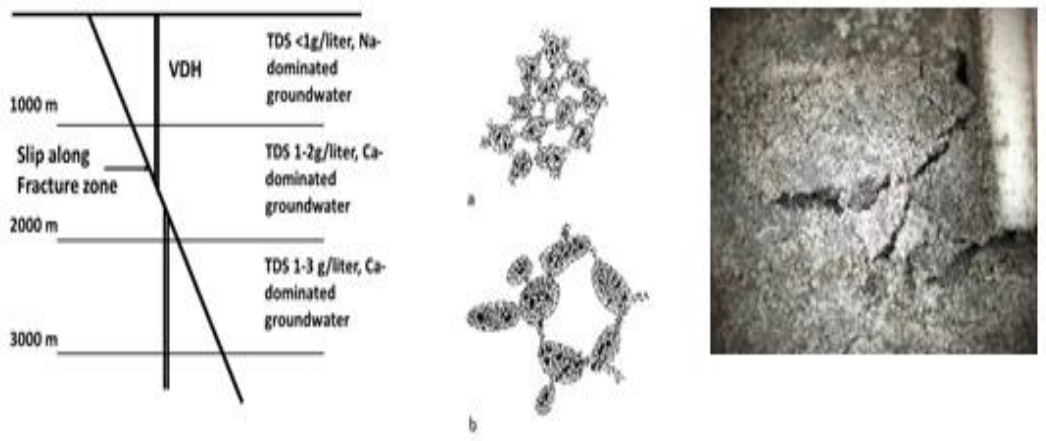

Figure 11: VDH affected by salt water and heat.
Left: Seismic/tectonic shearing of borehole in rock with typical salt zonation (TDS) of the groundwater.
Center: Schematic drawings of clay microstructure in a) low-electrolyte porewater and b) in salt porewater.
Right: Smectite seal sheared after hydrothermal treatment at 95ºC; Note the brittle behaviour (200X, LED light).

As to chemical impact, the effect of dissolved salts on the physical behaviour of mud is particularly important as illustrated by the different thickness of the interlamellar hydrates, and thereby the variation in thickness of the smectite particle shown in Table 2. The main effect of the coagulation indicated in center Figure 11b is the up to ten times higher hydraulic conductivity of salt clay for one and the same dry density.

The microstructural constitution of smectites of the most common type, i.e. montmorillonite, and of illite, being the primary product of chemically induced conversion, is illustrated by Figure 11. A simple method involving digital determination of the size distribution of the pores and the total pore area (P) in percent of the total area (T) of studied ultrathin microtome-cut sections has turned out to be suitable for microstructural characterization of clay materials in which the porewater has been replaced by diffusive exchange of acrylate. A recent step to directly correlate the microstructural constitution with soil mechanical properties including the hydraulic conductivity (Bouchelaghem and Pusch, 2017) in 2D has improved the interpretation of the micrographs and offered an accurate way of describing and interpreting them. One notices that the smectite particle density is significantly lower than the density of the illitic crystallites and that the size of the voids of the latter is higher, both effects causing the much lower hydraulic conductivity of the smectite (Figure 12).

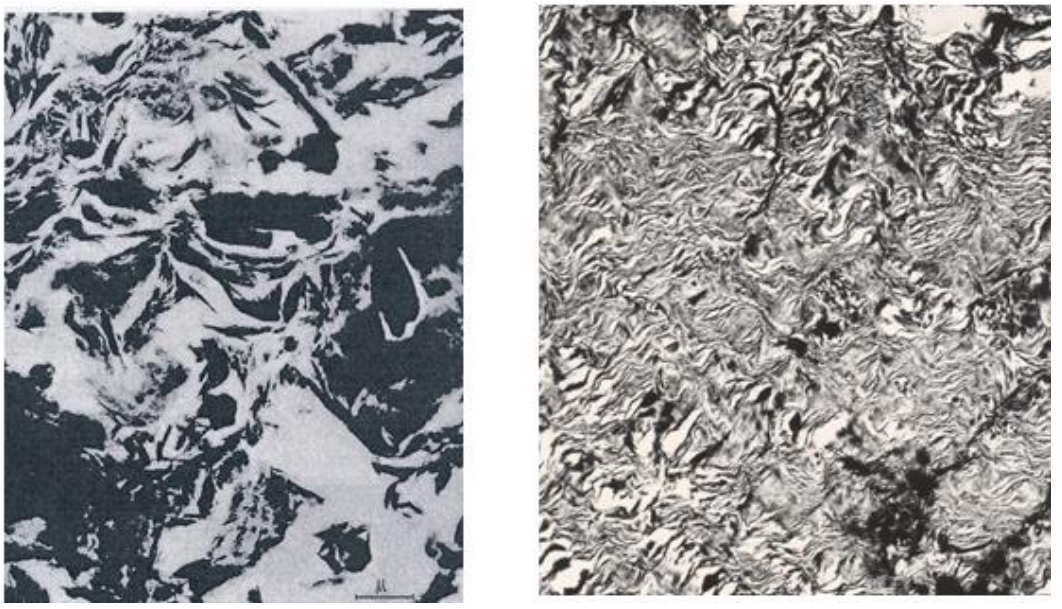

Figure 12: Transmission electron micrographs of illitic clay (left) and smectite-rich clay (right), both having 1,750kg/m^3 bulk dry density. Magnification indicated by the micrometer scale. Black represents minerals; white are sectioned voids.

Physically, any change in effective stress in clay causes densification or expansion and change of the dry density. Two processes have a bearing on the physical properties of clay seals and thereby on their waste isolation capacity: 1) Shearing of clay embedding supercontainers with or without HLW, as indicated in Figure 11 (left), which can take place along intersected natural weaknesses like fracture zones in the host rock, and 2) Settlement of supercontainers placed in deep boreholes. As to the first case, we will focus on the stress/strain/time performance of clay embedding supercontainers that controls the short- and long-term sealing potential of the continuous clay barrier established between concrete plugs in deep boreholes. The matter is long-term strain imposed on the clay by its own weight and by the weight of supercontainers, as well as by creep in the clay seals and in the surrounding rock mass caused by rock pressure. The basis of the theoretical treatment of the matters is treated first followed by considering the physical interaction of the clay seals and surrounding rock of bored holes.

3.6 Mechanical impact by shear and creep

Here, we dwell a little on shear-induced creep, being an important reason for deformation of clay seals and prefer here to apply stochastic mechanics referring to the Eyring[5]/Feltham[6] creep model, named after the creators. It can be described by considering the cubical clay element with side-length "L" in Figure 13 exposed to a shear stress that causes strain along an arbitrarily selected plane through the element.

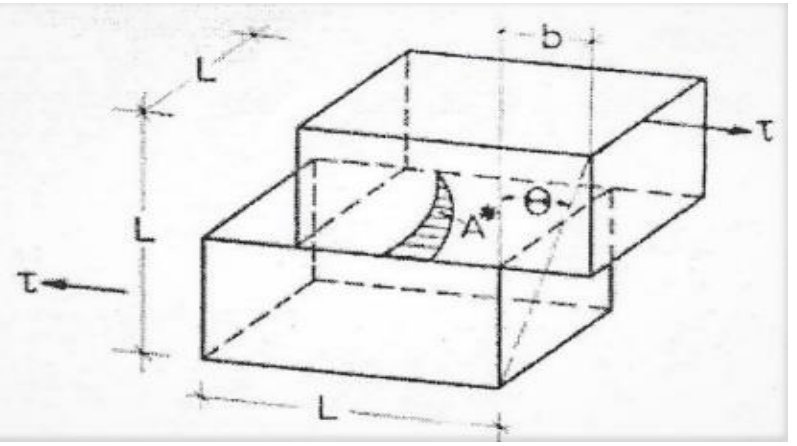

Figure 13: Clay element undergoing internal displacement caused by a slip unit jump generated by the local shear stress τ (Pusch and Feltham, 1980).

The passage of a slip through the element displaces the part above the slip plane by an amount "*b*" causing shearing by *b/L*. The model has the form of a time- and stress-dependent function controlled by the energy barrier spectrum on the molecular level. The evolution of strain depends on the energy required to overcome barriers representing the interparticle bond strength. This is a fundamental starting point for deriving stress/strain relationships that lead to practically useful models for predicting creep strain. Following Pusch and Feltham and assuming that interparticle slip has been activated at a certain point, meaning that an energy barrier has been overcome, a contribution to the overall shear strain occurs by the extension of local slip-patches. As explained below a linear stress/creep-rate relation holds for very low bulk stress levels, while at higher stresses the strain rate increases exponentially.

Shearing takes place by activation of barriers on the microstructural scale to slip. They form a spectrum as indicated in Figure 14 *(Right)*. As for most crystalline or pseudo-crystalline materials the spatial differences in barrier height forms a spectrum of interparticle bond strength representing a first-order variation, a second-order variation being represented by the interaction of differently sized particle aggregates. In coherent form these behave as strong units that remain intact

[5] cf. Eyring and Halsey, 1948
[6] cf. Pusch and Feltham, 1980

for small strain but yield at large strain and contribute to the bulk strength by generating dilatancy. The energy spectrum is hence not a material constant but changes with strain and thereby with time. An appreciable fraction of the strain-induced microstructural changes is preserved but exfoliated smectite stacks reorganize and cause self-healing by forming gels of different density depending on the available space and rate of strain. This means that local bond breakage is balanced by formation of numerous new bonds that make the altering microstructural network stay coherent for low and moderate bulk shear stresses, while higher shear stresses cause irreparable changes of the network leading to bulk failure at a certain critical strain.

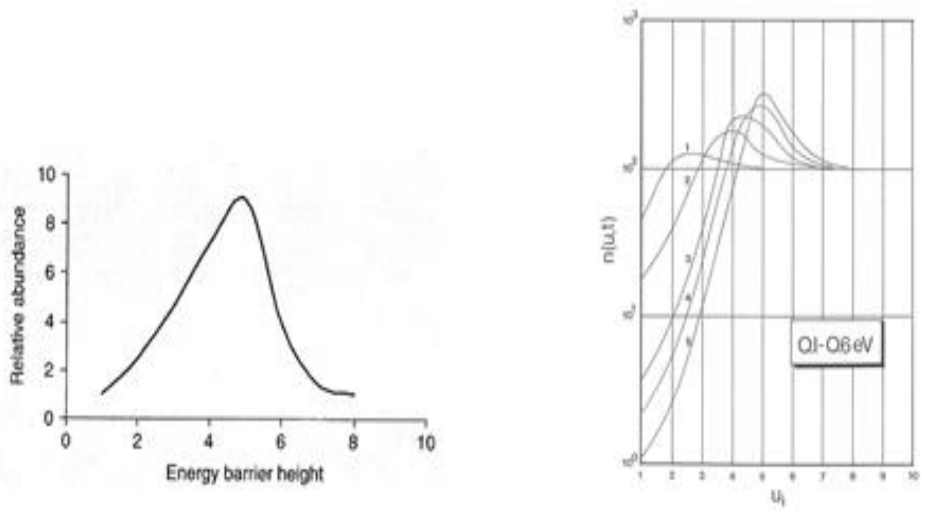

Figure 14: *Left*: Spectrum of energy barriers (eV) ranging from weak hydrogen bonds to primary valence bonds. *Right*: Change in energy barrier height distribution with time *t* at shear strain creep (*t*=6>*t*=5 etc).

The response of the structure to macroscopic shearing is that the overall deformation of the entire network of particles changes by disintegration, translation and rotation of weaker aggregates. Breakdown of aggregates that are transformed to assemblies of flaky particles is seen in Figure 15. It has been manifested by several electron microscopic studies (Pusch, 2019).

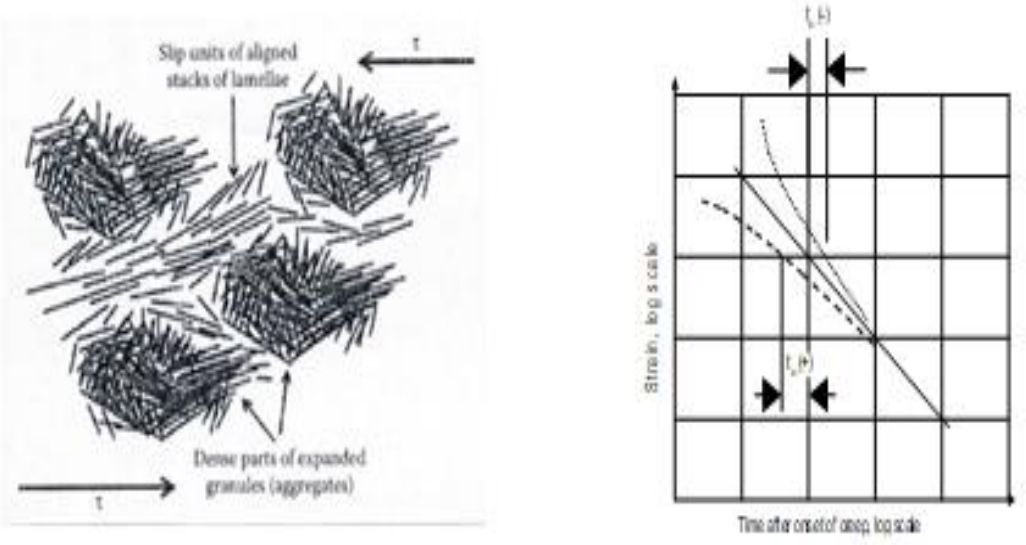

**Figure 15: Microstructural processes in creep of clay.
Left: Formation of slip domains by shearing of particle aggregates (Pusch, 2019). Right: creep curves of log time type showing exceptions from the theoretical mean curve shape for t_o=0. Negative t_o-values commonly imply brittle behaviour by cementation (Feltham, 1968).**

For a clay element subjected to a constant deviator stress one can assume that the number of energy barriers of height u is $n(u,t)\delta u$ where δu is the energy interval between successive jumps of a unit, and t the time, the entire process being stochastic. The change in activation energy in the course of evolution of strain means that the number of slip units is determined by the outflux from any u-level into the adjacent, higher energy interval and by a simultaneous inflow into the interval from u-δu. Each element of a clay seal contains a certain number of slip units in a given interval of the activation energy range and displacement of such a unit occurs as the shifting of a patch of atoms or molecules along a geometrical slip plane. In the course of the creep process the low energy barriers are triggered early and new slip units come into action at the lower energy end of the spectrum in Figure 16. This end represents a "generating barrier" while the high u-end is an "absorbing barrier". In principle, an increased deviator stress affects the rate of shift to higher u-values provided that shearing process does not significantly reduce the number of slip units. This is the case if the bulk shear stress does not exceed a certain critical value, which is on the order of 1/3 of the conventionally determined bulk strength. In principle this can be termed "primary creep".
For low shear stresses, allowing for "uphill" rather than "downhill" jumps one gets for the rate of change of $n(u,t)$ with time:

$$\delta n(u,t)/\delta t = \nu[-n(u+\delta u,t)exp[-(u+\delta u)/kT] + n(u,t)\exp(-u/kT)] \quad (2)$$

where:

δu=width of an energy spectrum interval; ν=vibrational frequency (about E11 per second); t=time; k=Boltzmann's constant; T=absolute temperature.

Using Eq.(3) and Feltham's transition probability parameter (Feltham, 1968) to describe the time-dependent energy shifts and assuming that each transition of a slip unit between consecutive barriers gives the same contribution to the bulk strain, one gets the bulk shear strain rate as Equation (3) with $t<t_o$ as boundary condition:

$$d\gamma/dt = B(1-t/t_o) \quad (3)$$

The appropriate constant B and the value of t_o depend on the deviator stress, temperature and structural details of the slip process. The creep and creep rate can hence be expressed by Equations 4 and 5:

$$\gamma = \alpha t - \beta t^2, \ (t<a/2\beta) \quad (4)$$

meaning that the creep starts off linearly with time and then dies out (cf. Figure 16).

For higher bulk loads, the strain on the microstructural level causes some irreversible changes associated with local breakdown and reorganization of structural units. But there is repair by inflow of new low-energy barriers parallel to the strain retardation caused by the successively increased number of slip units being halted by meeting higher energy barriers. This type of creep can go on for ever without approaching failure. Following Feltham, the process of simultaneous generation of new barriers and migration within the transient energy spectrum, lead to the expression for the creep shear rate in Equation 5:

$$d\gamma/dt = *A \int_{u2}^{u1} n(u,t)exp(-u/kT)du \ , \ (*A \text{ is a constant, cf. Figure 10}) \quad (5)$$

The implication of this expression is that the lower end of the energy spectrum mainly relates to breakage of weak bonds and establishment of new bonds where stress relaxation has taken place due to stress transfer from overloaded parts of the microstructural network to stronger parts, while the higher barriers are located in more rigid components of the structure.

Feltham (1968) demonstrated that for thermodynamically appropriately defined limits of the u-spectrum the strain rate appertaining to logarithmic creep takes the form of Equation 6:

$$d\gamma/dt = BT/(t+t_o) \quad (6)$$

where B=is a function of the shear stress τ, and t_o is a constant of integration, which leads to a creep relation closely representing the commonly observed logarithmic type, implying that the creep strain is proportional to $\log(t+t_o)$. The significance of t_o is understood by considering that in the course of applying a deviatoric stress at the onset of creep, the deviator rises from zero to its nominal, final value. A u-distribution exists at t=0, i.e, immediately after full load is reached, which we regard as equivalent to one which would have evolved in the material initially free from slip units, had creep taken place for a time t_o before loading. Thus, t_o is characteristic of the structure of the prestrained material (cf. Feltham, 1968; Pusch et al, 2011). Further increase in deviator stress leads to "secondary creep" in which the strain rate tends to be constant. Creep of critically high rate makes it impossible for microstructural self-repair: comprehensive slip changes the structure without allowing reorganization, which yields a critical strain rate that inevitably leads to failure. For smectite clay shear-induced formation of slip units, consisting of dispersed stacks of lamellae, is much more comprehensive than in illitic and kaolinite-rich in clays. The successive increase in the number of slip units implies an important self-sealing ability that causes attenuation of the creep even for high shear stresses as indicated by the diagrams in Figure 17, representing creep testing of smectitic clay (Pusch, 2019). Figure 17 (right) exhibits Newton-type flow at large strain.

The strain rate evolution shown in Figure 17 (right), leading to a nearly constant strain rate, was recorded after increasing the average shear stress from 6 to 23kPa, which was expected to cause instant failure. The strain-hardening effect was caused by re-grouping of dispersed dense particle aggregates to form a matrix of stacks of lamellae. This caused an increasing specific surface area with most of the shear resistance provided by a steadily increasing but ultimately constant number of quickly formed and broken hydrogen bonds like in viscous gels of colloidal matter. This suggests that smectite clays may not undergo failure like illitic clays, i.e. by slip along discrete failure planes, but deform to give zone failure using the appropriate soil mechanical term. The creep rate attenuated but turned into constant low strain rate without leading to failure in the two week long test.

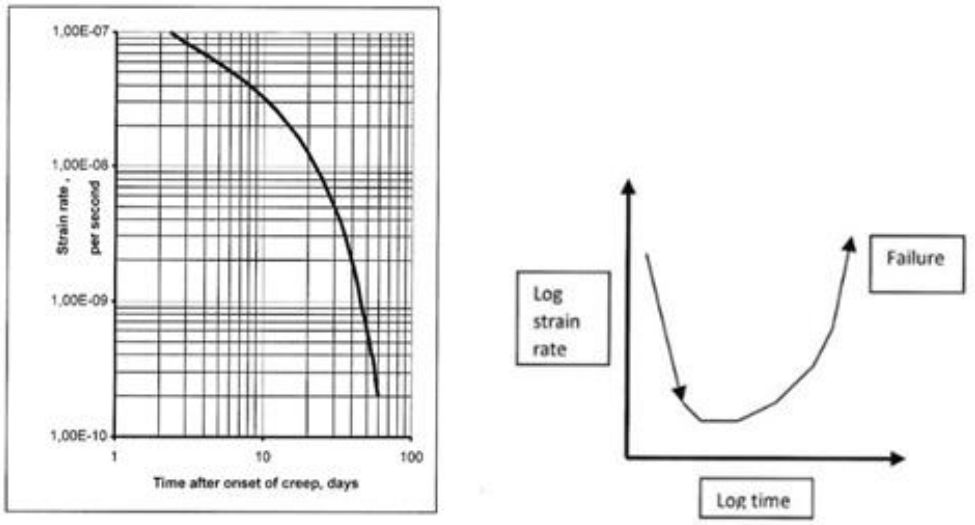

Figure 16: Creep strain rate of smectite-rich clay (MX-80) saturated with distilled water. Left: clay with 790kg/m^3 dry density under 6kPa average shear stress. Right: Typical evolution of failure.

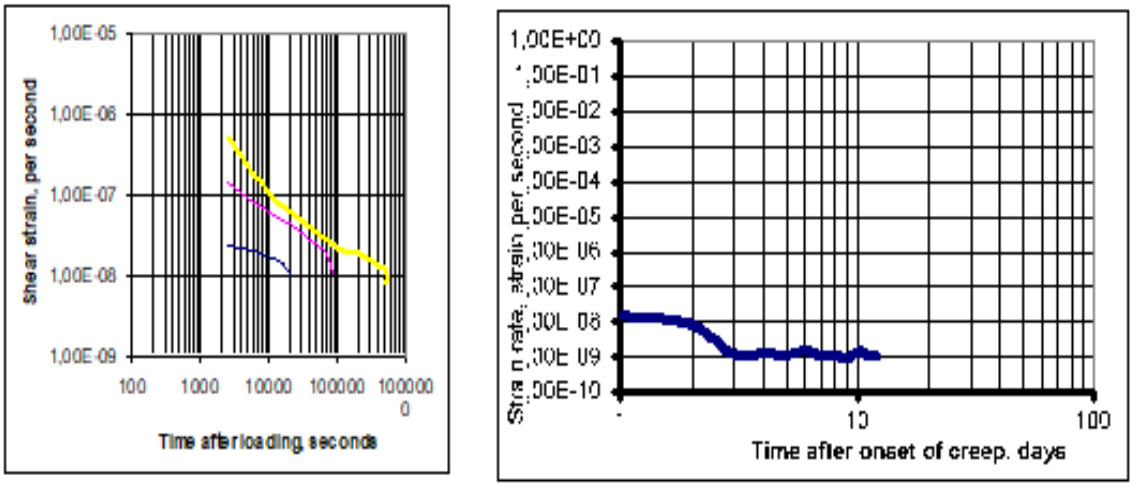

Figure 17: Creep strain rate of smectitic clay with dry density 1490kg/m^3 saturated with distilled water, and exposed to medium high shear stresses. Left: Average shear stresses 11, 23 and 39kPa (from top). Right: Nearly constant strain rate of the clay in Figure 16 exposed to 23kPa shear stress.

3.7 Settlement of waste-containers by creep in KBS-3V type smectite seals

Creep in smectite seals like canister-embedding matured clay can be important for preservation of its homogeneity after shearing or exposure to hydrothermal conditions. The theoretical basis of applied physical models is the same as already described and will be indicated here for identifying the major steps taken to solve the general problem of calculating the settlement rate of a 25ton supercontainer in deposition holes of KBS-3V type (Figure 18).

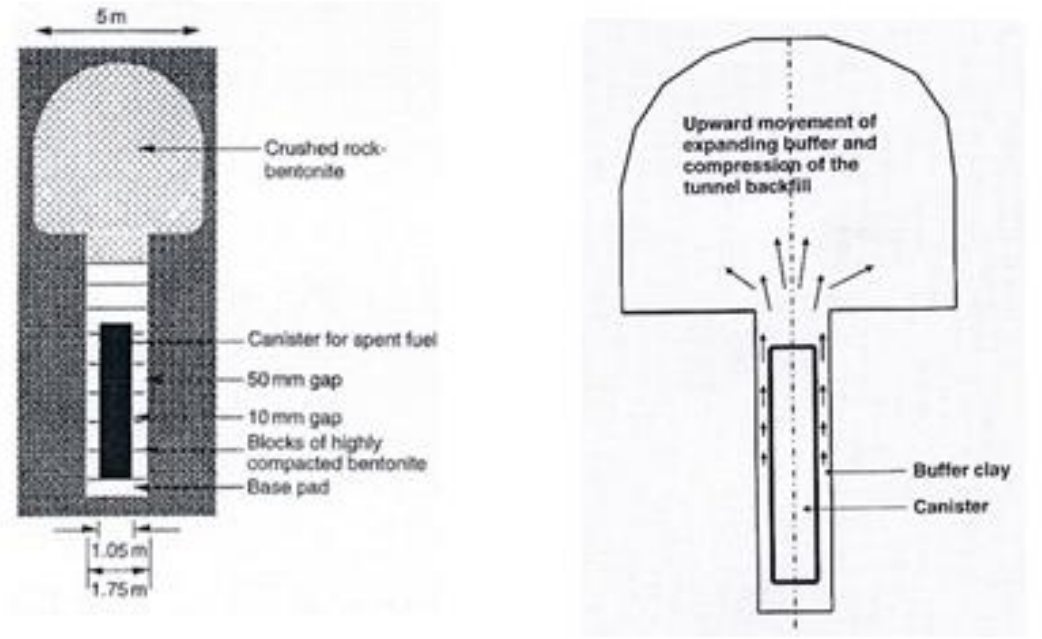

Figure 18: The original KBS-3V concept.
Left: Layout. Right: Axial tension of canister by upward expansion of the surrounding "Buffer" clay is a weakness.

The diameter and height of the canister was 1.05m and 4.8m, respectively. It was assumed to rest on a 0.5m thick block of dense smectite-rich clay, be surrounded by 0.35m of such clay and be covered by 1.5m clay, all confined in a bored hole with about 8m depth in rigid rock. The E-modulus of the clay was taken as 300MPa and Poisson's ratio as 0.49. Room temperature was assumed representing a few hundred years after waste disposal.

The settlement rate *ds/dt* at room temperature was predicted by use of Equation 7, which is a generalized version of Equation 6:

$$ds/dt = \beta \, T \, D \ln t \qquad (7)$$

β = creep strain parameter evaluated from undrained triaxial tests of smectite-rich clay with 1,590kg/m^3 dry density.

$D = \sigma_1 - \sigma_2$ (average deviator stress), where $\sigma_1 > \sigma_2 = \sigma_3$ are principal stresses with $\sigma_2 = \sigma_3$ are principal stresses assumed to represent also the swelling pressure. The results from the calculations are collected in Table 5 and Figure 19.

The boundary element (BEM) code BEASY (developed by Computational Mechanics Center (CMI), Southampton, England), which company also made the calculations, was used, taking the strain parameter β from undrained triaxial tests of montmorillonite-rich clay with a dry density of 2000kg/m^3, assuming room temperature (30^{o}C).

Table 5: Predicted settlement of full-scale KBS-3V canister at room temperature with and without slip along the contact between clay and rock and canister.

Time after onset of creep [sec]	Settlement with slip at contact [mm]	Settlement without slip at contact [mm]
E0	0.358	0.049
E1	0.426	0.058
E2	0.493	0.068
E3	0.560	0.077
E4	0.627	0.086
E5	0.695	0.095
E6	0.762	0.105

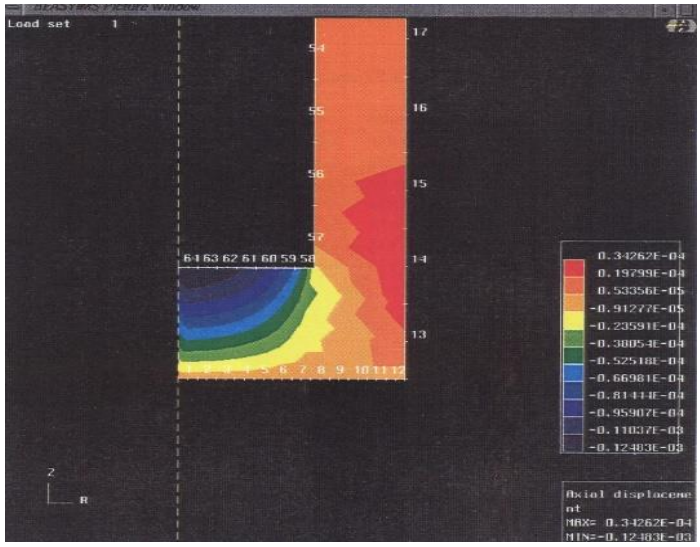

Figure 19: BEM-calculated distribution of the vertical displacements in the clay seal of KBS-3V after E6 years of loading assuming slip along the clay/cell and clay canister contacts (minus represents upward movement, plus is upwards), Pusch and Adey, 1986.

The calculated settlement, being significantly higher for the case with frictionless slip along the contact between clay and rock, will accordingly be about 0.4 to 0.5mm in 10-100 years. The rate of settlement then drops very rapidly and becomes ¾ of a millimeter in E6 years. In practice, the rate of settlement will be either slower because of the stiffening effect of cementing precipitated silicious compounds, or faster because of superimposed consolidation by compression.

Figure 20 shows a model VDH test for measurement of creep-generated settlement and predicted and recorded settlement of the model.

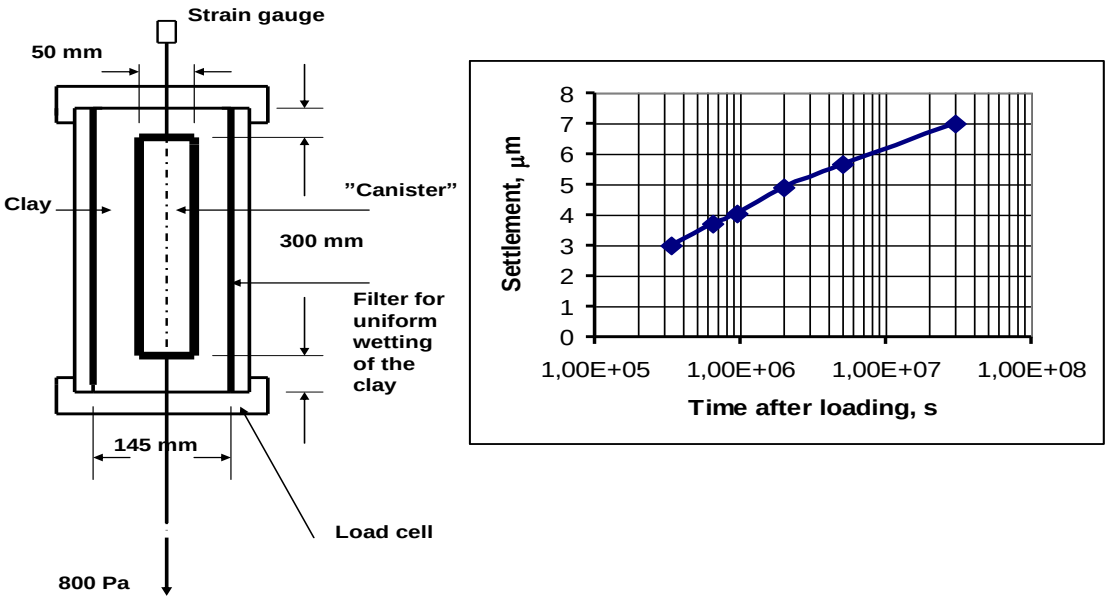

Figure 20: Experiment for measuring the settlement of a model canister embedded in clay. The test was made under drained conditions and an applied dead load of 800 N.

The 50mm diameter canister representing a weight of 80kg was loaded after about 3 months of maturation of the clay. The settlement was precision-recorded with an accuracy of E-4 µm. The load application caused 2-3µm visco/elastic settlement in the first few hours. The subsequent creep strain was about 6µm at the end of the 2 months long recording and about µm after 3 months as indicated by the diagram in Figure 20. It was approximately proportional to log time *t* with a slightly decaying trend.

The small-scale test clay block was made by compaction of smectite-rich smectite clay granules sized 0.01-0.2mm, and trimmed to fit in the load cell with access to distilled water via a filter for 3 months maturation leading to complete saturation at a dry density of 1590kg/m^3. The experiment was carried out under drained conditions after 3 months of maturation with access to distilled water from the filter-

equipped cell for microstructural homogenization. The same type of prediction of the settlement rate was made as for the KBS-3V case of a 25ton supercanister with HLW embedded in montmorillonite-rich clay with the same dry density, 2000kg/m^3 was performed. The calculations gave settlements that agreed well with the recorded ones as shown by Table 5.

Table 5: Predicted and real settlement of VDH model at 20ºC (cf. Figure 17).

Time after loading [sec]	Predicted settlement [μm]	Recorded settlement [μm]
3E5 (0.01 y)	3.0	3.0
6E5 (0.02 y)	4.0	3.7
3E6 (0.10 y)	5.0	5.2
6E6 (0.20 y)	6.0	6.0

One concludes from the data that the settlement by shear strain on the microstructural level is very small and of similar magnitude for both HLW disposal concepts, disregarding from initial canister movements related to strain generated at the installation of the various components.

3.8 Chemically caused changes in physical behaviour of clay seals

The basic issue is how long-term function of smectitic clay seals is affected by chemical processes in a HLW repository. Such processes involve mineral conversion from smectite to illite and cementation by precipitation of silicious and iron complexes.

A generally accepted empirical chemical process in the evolution of clay seals is defined by Equation 8:

$$S + (Fk + Mi) = I + Q + Chl \quad (8)$$

where *S* denotes smectite, *Fk* K-feldspars, *Mi* micas, *I* illite, *Q* quartz, and *Chl* chlorite.

The conversion formula is a generalization and says nothing about the ways in which alteration to illite takes place and what the conditions are for such change. Diagenetic formation of illite and interstratified I/S (illite/smectite) was an established process in the clay mineral society already in the sixties, implying layer-by-layer conversion of smectite layers to illite. Several investigators have shown that the conversion can have the form of dissolution of smectite and precipitation of (20Å) illite particles in intimate association with smectite particles. A most important parameter that does not appear explicitly in the equation is access to

potassium. It is generally believed that it determines the rate of illitization in salt clay environment and that the amount of illite formed will be insignificant where the concentration of this element is very low. The potassium concentration is significant in salt groundwater and appreciable in weathered clay in which potassium may originate from dissolved I/S particles, implying cannibalization. Naturally, conversion to illite is slower in very dense smectite clay than in soft clay, like bore mud, since the migration of all elements required for neo-crystallization takes place by diffusion to which there can be several obstacles.

The role of γ-radiation has been indicated in a joint French/Swedish project in which 7cm long MX-80 samples with a dry density of 1,650kg/m^3 were confined in cells with an iron plate at the heated end and a water saturated filter at the opposite end (Pusch et al, 1993; Pusch, 2008). Weakly brackish water with Na as dominant cation and <10ppm potassium was circulated through the filter being kept at 90^{o}C. The iron plate was heated to 130^{o}C during the 1-year long experiments, yielding a thermal gradient of about 6^{o}C/cm. The solution was pressurized to 1.5 MPa. In one of the tests a gamma radiation dose of about 3E7Gy acted on the iron plate, the adsorbed radiation dose being 3,972Gy/h at the hot plate, around 700Gy/h at half length of the sample, and 456Gy/h at the coldest end. The investigation of the samples comprised XRD analysis, electron microscopy with EDX, chemical analysis, infrared spectrometry IR, and CEC determination. Figure 21 shows the major changes in terms of XRD spectra:

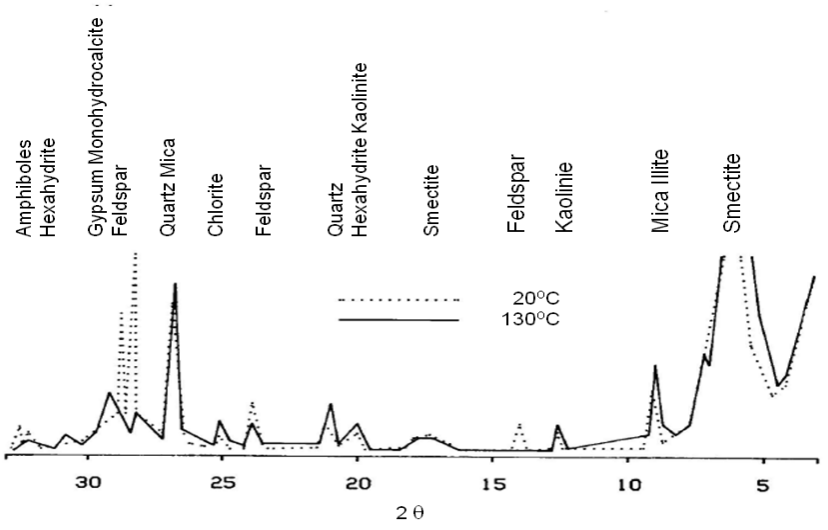

Figure 21: Schematic diffractograms of virgin smectite-rich clay at 20^{o}C and after 1 year of hydrothermal treatment (130^{o}C). Feldspars, amphibole, some of the quartz and smectite in virgin clay disappeared in the latter (dotted curves).

The analyses showed that there was almost no difference between the equally heated sample exposed to γ radiation and the one that was not irradiated[7], except that Fe migrated from the iron plate into the clay somewhat quicker under radiation. Comparison with "virgin" MX-80 clay showed that hydrothermal treatment with and without radiation gave insignificant chemical changes, which was also supported by CEC data. They showed that virgin MX-80 had CEC=99meq/100g while the most strongly heated and radiated clay had CEC=93meq/100g. However, creep testing at room temperature of samples from various distances from the hottest end gave witness of significant stiffening. Thus, the shear strain of the sample exposed to 130°C was about 3 times smaller than of the one heated to 90°C.

A chemical model proposed by Grindrod and Takase (1993) considers dissolution and precipitation of phyllosilicates, taking $O_{10}(OH)_2$ as a basic unit and defining a general formula for smectite and illite as:

$$X_{0.35}\, Mg_{0.33}\, Al_{1.65}\, Si_4O_{10}\, (OH)_2 \text{ and } K_{0.5\text{-}0.75}\, Al_{2.5\text{-}2.75}\, Si_{3.25\text{-}3.5}\, O_{10}(OH)_2 \quad (9)$$

where X is the interlamellar absorbed cation (Na) for Na montmorillonite.

Dissolution takes place according to the following reaction:

$$Na_{0.33}\, Mg_{0.33}\, Al_{1.67}\, Si_4O_{10}(OH)_2 + 6H^+ = 0.33Na + 0.33Mg^{2+} + 1.67Al^{3+}\, 4SiO_{2(aq)} + 4H_2O \quad (10)$$

while precipitation takes place according to the following reaction:

$$K\, AlSi_3\, O_{10}\, (OH)_2 = K^+ + 3Al^{3+} + 3\, SiO_2(aq) + 6H_2 \quad (11)$$

(logK being a function of temperature) in which we recognize the silicious precipitates.

The rate of reaction *r* can be expressed as:

$$r = A\exp(-E_a/RT)(K^+)S^2 \quad (12)$$

where:
A=coefficient
E_a=activation energy for S/I conversion
R=universal gas constant
T=absolute temperature
K^+=potassium concentration in the porewater
S=specific surface area for reaction

[7] The matter has been dealt with by Ewing et al [19] and others in parallel.

The kinetic reactions are linked with diffusion-dominated transport of involved aqueous species, i.e., silica, aluminum, sodium, magnesium, and potassium to form a set of quasi-nonlinear partial differential equations for the ion species and minerals. The modellers made spatial discretising by using a finite difference scheme that provided a set of ordinary differential equations by use of which one can determine the concentration of each species by solving the mass action equations for the total concentration of the element in question.

Grindrod and Takase applied their model to the KBS-3V case assuming the following data:

- dry density of the smectite buffer =1,700kg/m^3
- porosity =0.35,
- montmorillonite fraction by weight =75%,
- initial pore water is seawater,
- groundwater of seawater salinity assumed to be in equilibrium with granite at the specified temperature in the surrounding rock, *e.g.*, 60^{o}C during the first 500 years,
- temperature at canister surface=90^{o}C, temperature at rock wall=60^{o}C,
- diameter of hole is 1.8m, diameter of canister is 1.0m,
- vertical water flow rate in the 1cm pervious rock annulus (EDZ) around the hole is 1mm/day and 1mm/month, respectively,
- diffusion coefficient for K^+ in the clay is E-9m^2/s,
- considered time=500 years

Assuming the radial thermal gradient (about 0.75^{o}C per cm radial distance from the canister surface) to be constant during the considered time period, silica will be released and transported from the hottest to the coldest part of the clay seal. Application of the model shows that no illite would be formed in this period of time. However, as documented by extending the calculations to include a period after 500 years with a linear temperature drop with time to 25^{o}C after 10,000 years causes silicification and illite formation after 500 years, the first mentioned appearing in Figure 22, from which it was concluded that precipitation of quartz will take place within about 0.1m distance from the rock wall. The possibility of amorphous silica precipitation being formed is believed to depend very much on the time-scale of cooling relative to that of quartz precipitation. Rapid cooling leaves the system super-saturated with quartz, and the excess concentration of silica in solution eventually reaches the solubility of amorphous silica at the lower temperature. Illite may also have been formed in the hydrothermal experiments, at least in those conducted under open conditions, of which Figure 22 (*Right*) is an example.

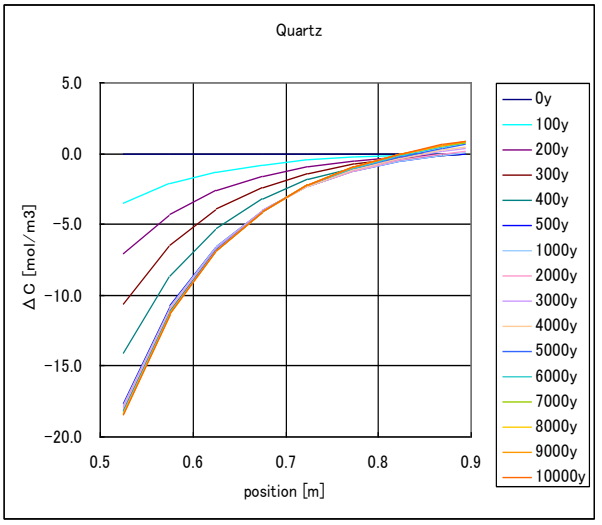

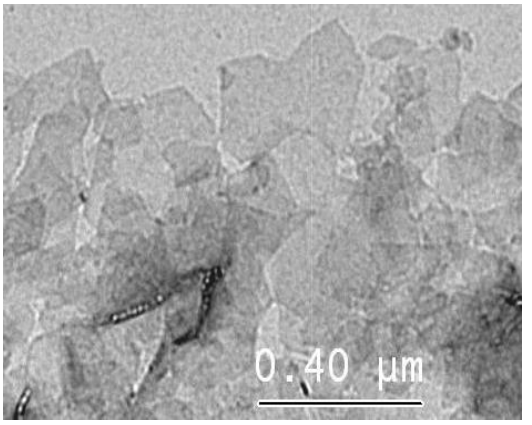

Figure 22: Evolution of quartz profile from start to 10,000 year) in smectite clay surrounding HLW at 90ºC in KBS-3V deposition hole. Left: Silica precipitation causing cementation in the outer, colder, 0.1m wide part of the clay (positions 0.8-0.9) and silica dissolution in the inner, hotter part (positions 0.8-0.9) according to Grindrod & Takase. Right: Neoformed illite in smectite-rich clay in 3-year field experiment (After Kasbohm).

Several hydrothermal field tests have offered evidence of chemical impact on smectite seals in SKB's two Swedish underground laboratories, the STRIPA and ÄSPÖ test sites, for determining changes in mineralogical composition and physical properties of smectitic clay under repository-like conditions. A general conclusion from these investigations of smectite-rich clay (Pusch et al, 2019) was that mineralogical changes as well as microstructural changes and cementation processes had been significant.

The hydraulic conductivity *K* was measured by applying hydraulic gradients of up to 4,000m/m, which were considered acceptable at that time but are nowadays known to give too low conductivity values because of consolidation effects. Samples with a dry density of 1,670kg/m^3 and percolated with low-electrolyte solution for simulating low to medium brackish Stripa groundwater, was exposed to a hydraulic gradient of 2,000m/m that gave *K*=5E-13m/s after 17 hours, 4E-13m/s after 28 hours and 2E-13m/s after 100 hours. This drop was concluded to be due to creep strain of the compressed smectite grains, and by flow-generated transport of fine particles causing clogging of microstructural "channels", which combined to cause underestimation of the hydraulic conductivity[8]. The sample was

[8] In a recent percolation test of dense GMZ clay (Xiaodong et al, 2011) being a primary Chinese

then allowed to expand to a density of 1.510kg/m^3 and to homogenize, after which a hydraulic gradient of 400m/m was applied, giving *K*=E-13m/s after 141 hours. The swelling pressure of the sample used for determination of the hydraulic conductivity was recorded and found to be 50MPa for 1,670kg/m^3 dry density, 4.6MPa for the dry density 1,510kg/m^3, and 0.5MPa for the dry density 1,270kg/m^3 are in reasonable agreement with data for virgin montmorillonite

3.9 Cementation by precipitation – the most alarming threat to clay seals

The strongest threat of losing the ductile behaviour and potential of self-repair of smectitic clay seals is precipitation of silicious cementing agents originating from conversion of such clay to illite since it implies loss or strong reduction of the swelling potential of smectite seals. It can have the form indicated in Figure 23 that shows generalized smectite microstructure in virgin clay to the left and alteration to a denser state of the stacks of clay particles to the right. Cementing precipitations of crystalline or amorphous quartz, cristobalite and illite bind clay lamellae and small aggregates together and preserve the increased porosity and shear strength. This mechanism has been identified in various clays of smectitic origin as illustrated by the figure.

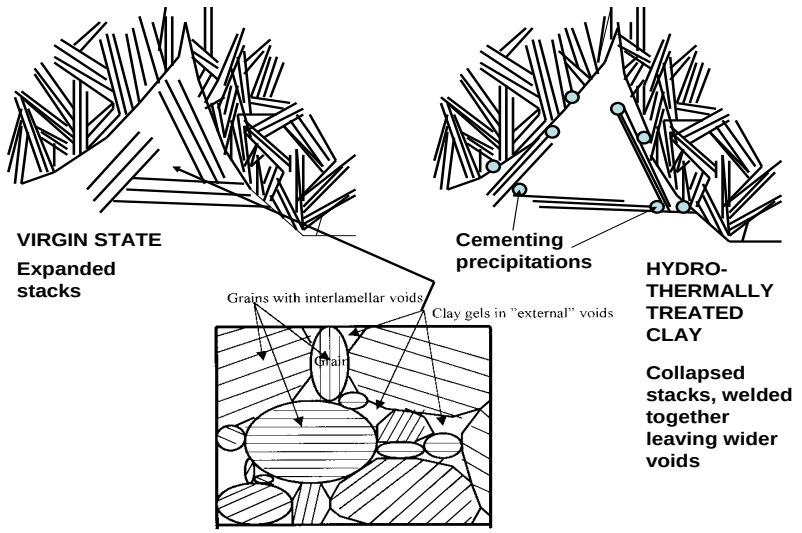

Figure 23: Growth of voids by heating and increased stiffness by cementing silicious precipitations. The small picture shows the clay grains before maturation in the form of dispersion of smectite particles and fixation of them by silicious precipitation (Pusch et al, 2011).

Buffer candidate comparable with MX-80, under a gradient of 60m/m for several days the evaluated hydraulic conductivity dropped to less than 1/100 by raising the gradient to 6,000m/m.

The Grindrod/Takase model predicted initiation of silicification and illite formation after 500 years within about 0.1m from the rock wall (cf. Figure 24), while amorphous silica would not be precipitated. The possibility of amorphous silica precipitation is believed to depend very much on the time scale of cooling relative to that of quartz precipitation. Rapid cooling would leave the system super-saturated with quartz, and the excess concentration of silica in solution would eventually reach the solubility of amorphous silica at the lower temperature. Application of the model to the deepest part of the deployment zone indicates comprehensive silicification (Figure 24) and very significant stiffness of the clay. After a few decades the entire clay seal system in the deployment zone would be expected to turn to claystone or argillaceous shale similar to the Ordovician bentonites at Kinnekulle in Sweden (Pusch and Madsen, 1995).

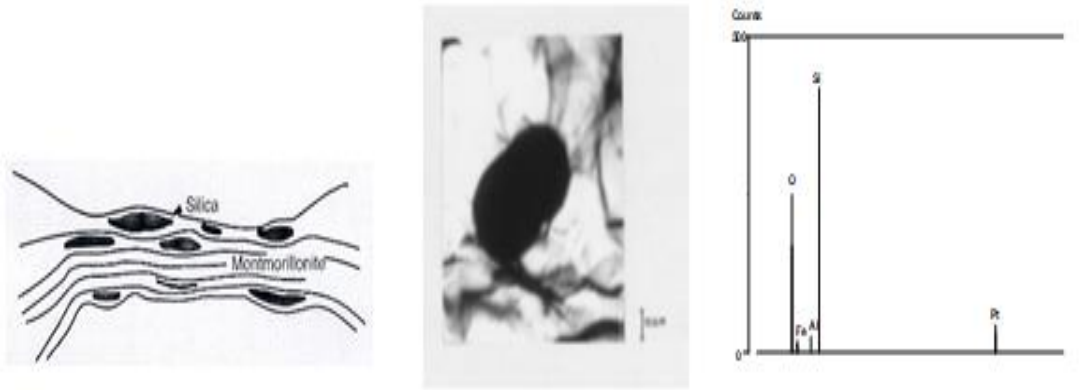

Figure 24: Silicious precipitations in deep clay layers.
Left: Distribution of precipitated silica in deep ocean clay layers (Nadeau and Bain, 1986). Center and right: Silica precipitation in pure montmorillonite hydrothermally treated at 150ºC, and spectroscopic analysis of the precipitate (Gueven, 1990).

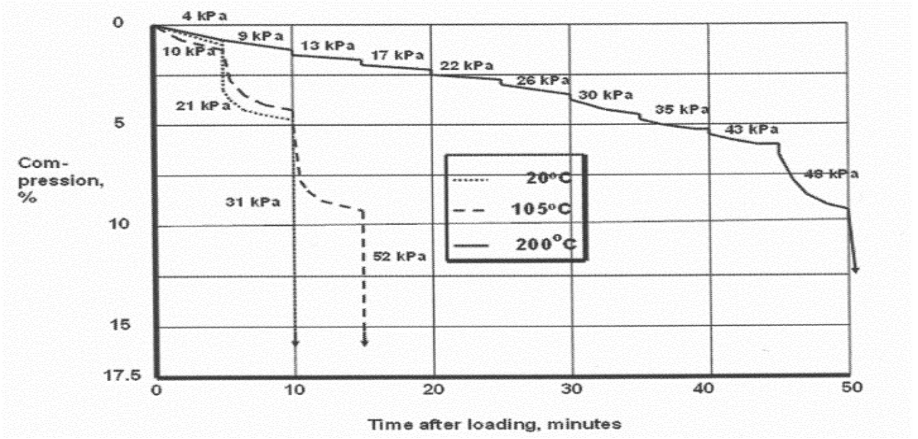

Figure 25: Unconfined, stepwise performed compression tests of freshwater saturated montmorillonite-rich clay with 1,650kg/m^3 dry density (Pusch, 2011). Slight stiffening took place of the specimen autoclaved at 105°C but became very significant in the sample exposed to 200°C.

An alternative chemical model that sheds further light on illitization has been forwarded by Kasbohm et al (2005) It fits the results from field tests made in SKB's ÄSPÖ underground laboratory where MX-80 clay was used. XRD and chemical analysis using TEM-EDX technique were applied for determining whether mineralogical changes had taken place in the KBS-3V type field experiment (Pusch, 2008) causing the increased hydraulic conductivity of the aforementioned R8:225 sample. The main results from the mineralogical analyses are summarized in Table 6. The data were derived from comprehensive (>100 specimens) particle-wise TEM-EDX-measurements.

Table 6: Parameters from mineral formula per [$(OH)_2$ O_{10}]; Data from TEM-EDX-analyses (After Kasbohm).

Parameter	Virgin MX-80	R8:225: At Canister (90ºC)
Phases Traces:	Montmorillonite (low-charge montmorillonite), diVS-ml IS-ml, PSV-ml	Montmorillonite (low-charge montmorillonite), diVS-ml IS-ml, KSV-ml, 'albite'
Smectite Layers (S%), S% in IS-ml phases S% in diVS-ml	 85 % 90 %	 95 % 80 %
Interlayer charge (average of all)	0.222	0.305

Legend: IS-ml – illite-smectite mixed layer phases; diVS-ml – dioctahedral vermiculite-smectite mixed laaer phases; PSV-ml – pyrophyllite-smectite-dioctahedral vermiculite mixed layer phases; KSV-ml – kaolinite-smectite-dioctahedral vermiculite mixed layer phases.

Kasbohm's major findings from his investigations of clay seals in SKB's tests of smectite clay seals in a KBS-3V repository were:

- MX-80 clay contains two types of montmorillonite: i) montmorillonite with normal charge as end member of an IS-ml series, and ii) low-charge montmorillonite as end member of diVS-ml series. The ratio IS:diVS varies from 1/20 to 2/3.
- The R8:225 clay sample being located in contact with a 90ºC copper canister throughout the hydrothermal treatment had undergone substitution of Al^{3+} by Fe^{3+} in the octahedral layer causing higher lattice stresses because of the larger ion radius of Fe^{3+} than of Al^{3+}, thereby reducing the resistance of the montmorillonite to dissolution. The change in chemical composition of the montmorillonite is illustrated by the derived formulae:
    a. montmorillonite as end member of IS-ml series in virgin MX-80:

$$Ca_{0.04}\,Mg_{0.09}\,K_{<0.01}\quad Al_{1.64}\,Fe^{3+}_{0.13}\,Mg_{0.23}\,Ti_{<0.01}\,(OH)_2\quad Si_{3.96}\,Al_{0.04}\,O_{10}$$

    b. montmorillonite as end member of IS-ml series in hydrothermally treated clay:

$$Ca_{0.07}\,Mg_{0.02}\,Na_{0.04}\,K_{0.07}\quad Al_{1.46}\,Fe^{3+}_{0.23}\,Mg_{0.25}\,Ti_{0.03}\,(OH)_2\quad Si_{3.98}\,Al_{0.02}\,O_{10}$$

- The R8:225 clay had been step-wise altered from normally charged to low-charge montmorillonite by replacement of original Mg by Al. The composition of the montmorillonite as end member of diVS-ml series in the hydrothermally treated clay has the following form:

c. $Ca_{0.02}\ Mg_{0.04}\ Na_{0.01}\ K_{0.03}\quad Al_{1.62}\ Fe^{3+}_{0.16}\ Mg_{0.17}\ Ti_{0.04}\ (OH)_2\quad Si_{3.99}\ Al_{0.01}\ O_{10}$

- Montmorillonite was the dominating mineral phase in both virgin and hydrothermally treated clay. However, mineralogical changes induced by the hydrothermal conditions were obvious as indicated by an increase in smectite layer frequency in the IS-ml phases of the heated clay (95%) compared with the typical number for virgin MX-80 (85%), and by an associated drop in smectite layer frequency in the diVS-ml phases from 90% of the virgin MX-80 to 80% in the heated clay.
- The lower interlayer charge of R8:225 than of virgin MX-80 means, according to classical double-layer theory, that it should have higher swelling pressure, which is in agreement with the diagrams in Figure 26.

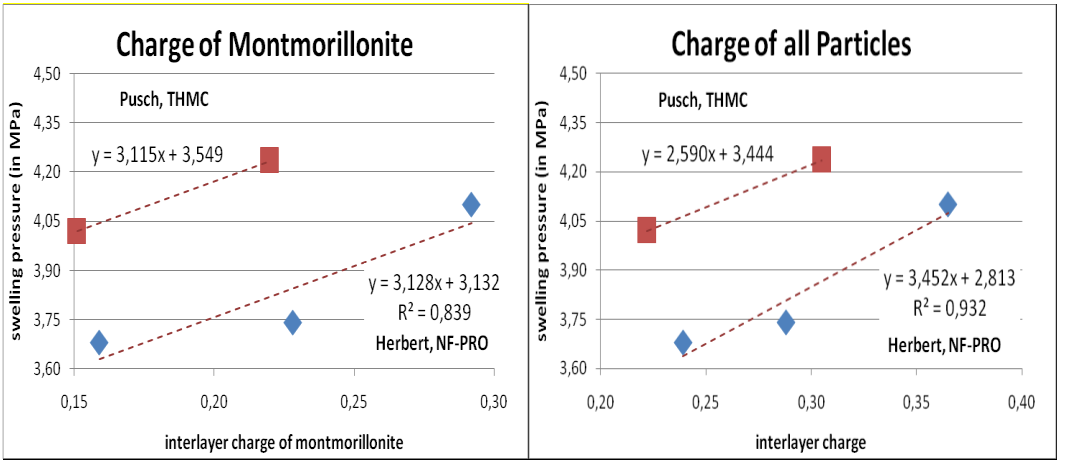

Figure 26: Comparison of swelling pressure vs. charge of MX-80 clay showing the same trend of increased pressure for increased charge in experiments using different techniques (After Kasbohm et al, 2005).

The reaction rate equation shows that silica will be released and transported from the very hot clay surrounding the canisters and be precipitated in the colder clay at the borehole wall (cf. Grindrod and Takase, 1993). Hence, assuming linear temperature drop with time back to 25°C in 10,000 years, illitization will be initiated early in the hottest clay while stiffening and loss of self-healing by cementing precipitates is expected near the rock, proceeding somewhat slower.

Log-time creep behaviour of dense montmorillonite-rich clay for medium-high shear stresses has been frequently recorded in laboratory and bench-scaled investigations like the study by Al Taie, 2014. The study gave examples of the rate of compression at uniaxial unconfined load tests as plotted in the diagram in Figure 27, which also shows the compression rate of undisturbed illite-rich clay of approximately the same density (cf. Table 5). The shear strain rate of illite was initially much higher than that of the smectite but dropped to about the same value

as for smectite when the multitude of "reserve" bonds in the smectite had been activated. The rate of strain of the illite had then become controlled by the very high "interparticle" friction in this clay.

Table 5: Geotechnical data of natural clays rich in illite, sampled from glacial clay in the Köping area in Sweden (Pusch, 1961). τ_{fu}=undrained shear strength, S_t =Ratio of virgin and remolded shear strengths.

Test	τ_{fu}, kPa	S_t	w, %	w_P	w_L	Organic content, %	Content of minus 2 mm particles, %	Preconsolidation pressure, kPa
1	18.8	7.6	70.3	20.1	85.4	3.5 %	50	12.5
2	12.9	8.0	71.8	15.9	96.4	3.5 %	34	8.6

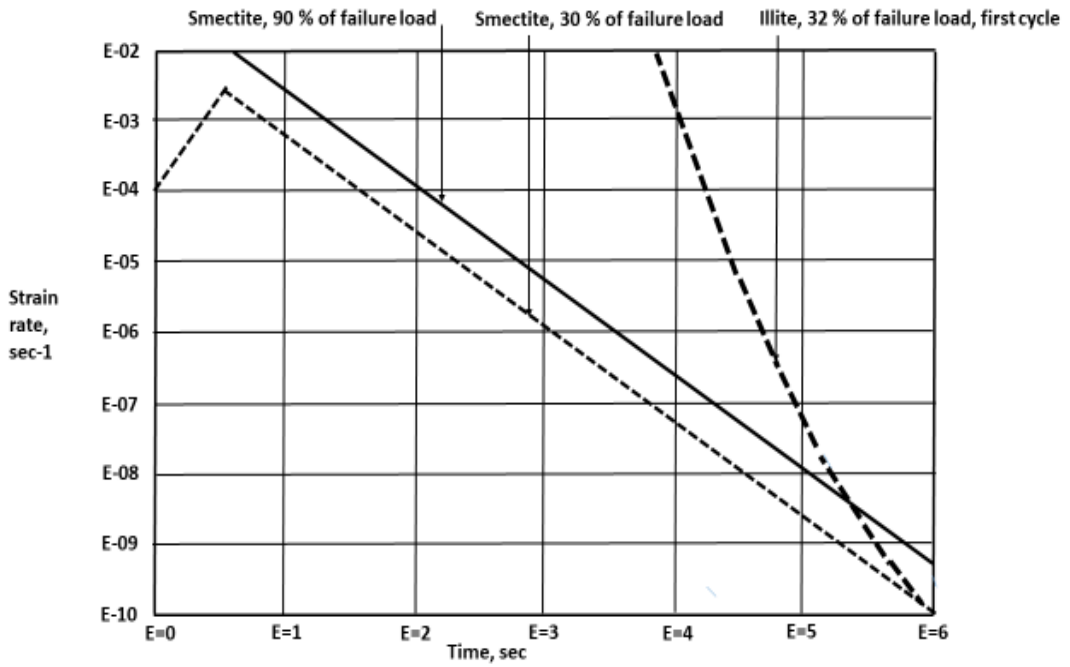

Figure 27: Creep strain rates of clays with dry density 1,600kg/m^3 and about 65% smectite content and about 65% illite, respectively. The percentages refer to the fraction of the conventionally determined undrained shear strength of the clays (Al Taie, 2014).

For VDH, the high temperature in the waste-bearing part causes a higher rate of illitization than in the upper part. Thus, using Equation 12, one finds that an increase in clay temperature from 100 to 150^{o}C speeds up the rate of conversion of montmorillonite to illite considerably: half the entire original content of montmorillonite will be converted to illite about 100 times quicker at the higher temperature than at 100^{o}C, assuming the activation energy to be 27kcal/mole and all other factors being the same. The strongest loss in effective sealing potential will

take place in the first 100 years but the practical importance is rather small since the waste-isolating ability of the clay reaction products is still considerable. Hence, for montmorillonite with a dry density of 1,600kg/m^3 converted to pure illite, the hydraulic conductivity will still be low, i.e. <E-8 m/s (Pusch, 2015). Complete conversion to non-expandable illite of the dense smectite clay in a supercontainer representing (2000kg/m^3 of solid clay) would take 100,000 years because the controlling mechanism is the very slow diffusive transport of potassium from the surrounding rock (Pusch, 2008).

4. Physical interaction of clay seal and confining rock

4.1 Role of host rock for long-term improvement of the waste-isolating capacity of clay seals in deep boreholes

An extra waste-isolating capacity of very deep holes against leakage of radioactively contaminated water in the deployment zone of deep holes can be gained by creep generated in the rock surrounding such holes (cf. Pusch et al, 2019). These investigators used the Kelvin rheological model (Figure 28), calibrated by a thermodynamically founded creep model termed "Eyring/Feltham creep model" worked out by Feltham and colleagues in the seventies as cited here.

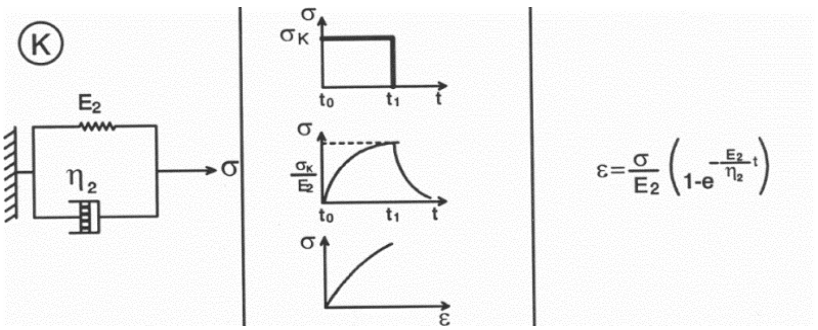

Figure 28: The original Kelvin rheological model.

Here, we will investigate whether the radial movement of the deep borehole walls resulting from creep in the surrounding rock can maintain tight contact between the clay and the rock and even improve the sealing effect of the clay by consolidation under the radial pressure generated by creep in rock. The following steps are taken in application of the model:

- The stress changes caused by creating deep holes by boring give a radial movement *u* that can be calculated by using the theory of elasticity: $u=pa(1-\nu)/E$ where $E=\sigma/\varepsilon$ and ν is Poisson's ratio, taken to be 0.2 here,

- For finding the time-dependent radial displacement of the borehole walls we will use the expression for strain of the Kelvin model, where the modulus of

elasticity of spring E2 in Figure 28 is taken as E4MPa and the dashpot viscosity as η=E20Pas for crystalline rock of ordinary quality, and assuming an E-modulus of E3MPa, and a dashpot viscosity of η=E17Pas for argillaceous rock. The periods of time for creep to develop are taken as 1 to E4 years. The assumed loading case implies that the pressure against the borehole walls is raised from an initially very low value when the dense clay is just being inserted in clay mud in the holes, to 4MPa within a year when the clay system has largely matured and stays so until the convergence of the holes has lasted for up to E5 years,

- The convergence can be defined as:

$$\varepsilon(t) = \frac{\sigma}{E}\left(1 - e^{-\frac{E}{\eta}t}\right) \tag{13}$$

where σ is Hooke`s stress, $E$ is Young`s modulus of the rock, η is the viscosity of the rock and t is the starting time of the creep. The time-dependent values of ε are used to calculate and to use these to calculate a corrected $E-$modulus, $E´$, by imposing:

$$E´(t) = \frac{p}{\varepsilon(t)} \tag{14}$$

Here, p is the rock stress, which is related to the Hooke´s stress by putting:

$$\sigma = p\left(1 + \frac{a^2}{r^2}\right) \tag{15}$$

In the present case one can take a to be the radius of the borehole, and $\sigma = 2p$. When the corrected Young´s modulus is at hand, one can calculate the time dependent radial displacement of the wall of the holes as:

$$u(t) = pr\frac{(1-\nu)}{E´(t)} = pr\varepsilon(t)(1-\nu) \tag{16}$$

One observes that use of Equation 16 is redundant, since $\frac{p}{E´(t)}$ equals $\varepsilon(t)$.

The calculated radial movement of the walls of an unfilled 800mm diameter borehole in typical crystalline rock at 2 and 4km depth using the Kelvin rheology model, is given by the graph in Figure 29.

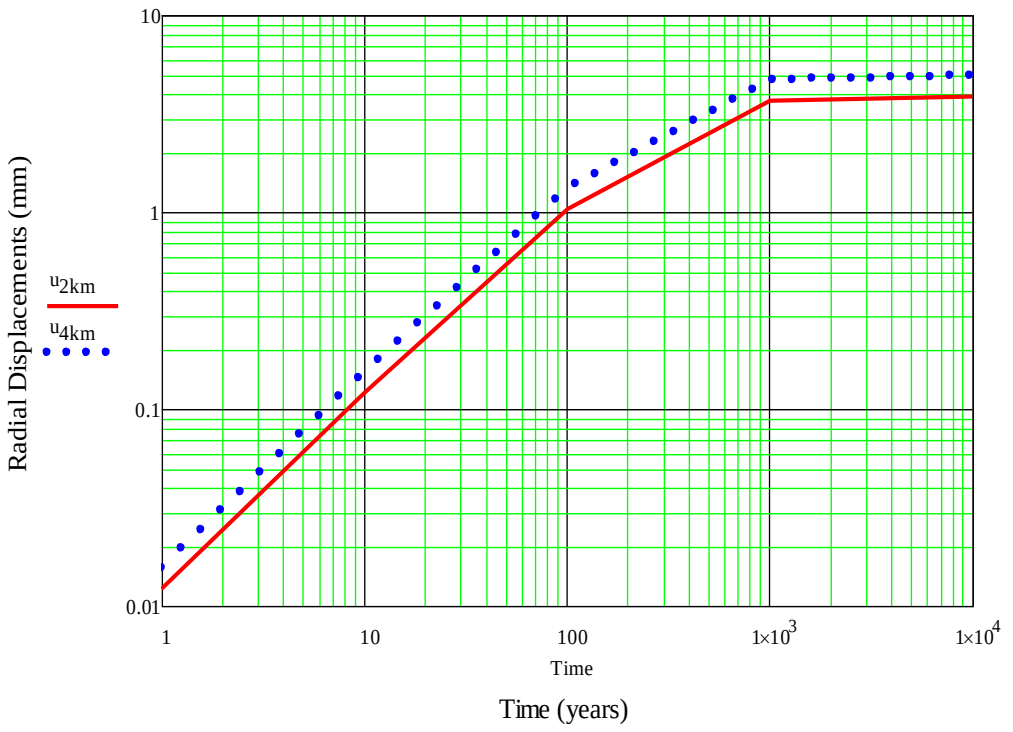

Figure 29: Calculated radial movement of the walls of an 800mm diameter borehole in typical crystalline rock at 2 and 4km depth according to the calibrated model. Impact of temperature neglected.

One finds that for VDH in crystalline rock of granitic type the radial inward movement of the lower, waste-bearing part of the 800mm hole after E2 years will be about 1.5mm, 5mm in E3 years, and 6mm in E4 years. For the upper part of the hole, where the rock pressure is lower, the corresponding movement will be about 1mm after E2 years, 3.5mm in E3 years and 4mm in E4 years neglecting the counteracting pressure exerted by the clay. The temperature rise to around 150°C in the lower part will increase the strain by about 0.1% and hence displace the borehole wall radially by about 1mm in the first hundred years after which further impact of heat becomes negligible.

For argillaceous rock with the representative rheological parameters one finds that the lower, waste-bearing part of the hole will have moved by about 100mm after E4 years and already after 100 years the displacement is very significant, i.e. 60mm.

4.2 Conclusive remarks concerning hole convergence

Using the Kelvin rheological model for calculating the radial convergence of very deep clay-sealed holes located in crystalline rock, it is found that the very small convergence of the considered 800mm diameter holes causes a negligible pressure on the clay. Thus, the calculations show that the maximum expected radial movement of the borehole wall in the first 500 years will be 2.5mm at 2km depth

and 3mm at 4km depth, which will only cause an increase in dry density of the clay from 1,600kg/m^3 to about 1,620kg/m^3. This will raise the swelling pressure from the assumed 4.0MPa to 4.1MPa and thereby reduce the hydraulic conductivity from 7E-12m/s to 4E-12m/s. In a 10,000 year perspective the wall of the holes at 4km depth will have moved towards their centers by 5mm and thereby increased the dry density to 1,640kg/m^3, which will raise the swelling pressure to nearly 4.2MPa and reduce the hydraulic conductivity to about 2E-12m/s. None of the changes will significantly affect the sealing potential of the clay seals. In an even longer perspective, like a hundred thousand year period, some further minor increase in density is expected, generating slightly better sealing function of the clay. However, parallel to this process chemically induced conversion of the smectite clay minerals to less expanding ones (illite) will take place and create an approximately tenfold permanent increase in hydraulic conductivity and a significant reduction in swelling pressure.

5. Discussion and conclusions

The key questions in assessing the waste-isolating capacity of dense smectite clay in the two considered concepts for long-term isolation of HLW from the biosphere: disposal in relatively shallow bored deposition holes and placement of such waste in very deep boreholes termed VDH, are 1) installation of clay seals, and 2) long-term isolation with special respect to the capacity of the clay seals to retain a sufficiently large part of their ductility and potential to self-heal after mechanical and chemical impact. A distinction has been made between the potential of smectite seals in shallow deposition holes of KBS-3V type and in very deep VDH holes.

5.1 Clay isolation offered by KBS-3V type concepts

This type of concepts come under the heading of mined repositories with relatively fast percolation of the clay seals because of significant hydraulic conductivity and gradients in the pervious host rock. This causes early changes in hydraulic conductivity and cementation of clay seals. Movements in the rock mass can cause significant shear strain in clay seals and HLW canisters hence causing risk of strain that can cause early and comprehensive rock fracturing and risk of leakage of radioactively contaminated water that can reach up to the biosphere.

5.2 Clay isolation offered by VDH-type concepts

- The lack of significant vertical hydraulic gradients makes installation of HLW and protecting smectite clay seals relatively easy. The isotropic stress conditions in the rock at large depth implies very low permeability, minimal mechanical disturbance, and low risk of shear strain in clay seals and in supercontainers provided that site investigations have made it possible to avoid intersection of the deep holes for HLW disposal and hydraulically and mechanically important fracture zones.

- Use of experimental data from extensive field investigations in underground laboratories have confirmed the applicability of models for numerical calculation of the homogenization of clay seals and estimation of the chemical effects taking place in all parts of very deep holes for HLW disposal.
- Use of rheological models developed from the classic Kelvin model complemented by a model representing rate process theory and stochastical mechanics is judged to be applicable for solving the problem of predicting over short and long time the convergence of deep bored holes for storing highly radioactive waste like spent reactor fuel. The application included determination of possible impact of the convergence of the holes on the constitution and properties clay seals placed in the holes. Deep deposition holes in argillaceous rock may offer the most suitable solution.

5.3 General estimate concerning clay isolation of HLW

The KBS-3V type concept and the deep VDH concept are believed to be constructible and to perform acceptably for sufficiently safe isolation of HLW for hundreds and thousands of years. The latter concept is however judged to work significantly safer and longer than the KBS-3V version because of the extra safety provided by the heaviness of deep groundwater and it is also estimated to be cheaper than a KBS-3V repository. Both concepts should be examined in more detail before final decisions are taken concerning design and construction.

References

[1] Taie, A. (2014). Performance of clay liners in near-surface repositories in desert climate. PhD Thesis, Luleå University of Technology, Sweden.

[2] Bouchelaghem,, F. and Pusch, R., (2017). Fluid flow and effective conductivity calculations on numerical calculations on numerical images of bentonite microstructure, Applied Clay Science, 144, pp.9-18.

[3] Brady, P.V., Arnold, B.W., Freeze, G.A., Swift, P.N., Bauer, S.J., Kenney, J.L., Rechard, R.P. and Stein, J.S. (2009). Deep borehole disposal of high-level radioactive waste. US Department of Energy, Washington DC.

[4] Eyring, H. and Halsey, G. (1948). The mechanical properties of textiles – the simple non-Newtonian model. High Polymer Physics, Chemical Rubber Co., Cleveland, Ohio pp.61-116.

[5] Feltham, P. (1968). A stochastic model of creep. Phys.Stat. Solidi, 30, pp.135-146.

[6] Grindrod, P., and Takase, H. (1993). Reactive chemical transport within engineered barriers. In: Proc. 4th Int. Conf. on the Chemistry and Migration Behaviour of Actinides and Fission Products in the Geosphere, Charleston, SC USA, 12-17 Dec. Oldenburg Verlag 1994, pp. 773-779.

[7] Gueven, N., Carney, L.L. and Ridpath, B.E. (1987). Evaluation of geothermal drilling fluid using commercial bentonite and a bentonite/saponite mixture. Sandia Nat. Lab., Albuquerque, Contractor Report, SAND86-7180.

[8] Kasbohm, J., Henning, K.H. and Herbert, H.J. (2005). Short- and long-term stability of selected bentonites in high-saline solutions. International Symposium on Large Scale Field Tests in Granite, Sitges, Barcelona, Spain November 12-14, 2003. Code 88404:231-240.

[9] Laith, A. T. (2014). Performance of clay liners in near-surface repositories in desert climate. PhD thesis, Luleå University of Technology, Luleå, Sweden.

[10] Nadeau, P.H. and Bain, D.C. (1986). Distribution of precipitated silica in deep clay layers. Composition of some smectites and diagenetic illitic clays and implications for their origin. Clays and Clay Minerals, 34 (455.464).

[11] Pusch, R, and Feltham, P. (1980). A stochastic model of the creep of soils. Géotechnique 30, 4. (497-506).

[12] Pusch, R. and Adey, R. (1986). Settlement of clay-enveloped radioactive canisters. Applied Clay Science 1 (253.365).

[13] Pusch, R. (1994). Waste disposal in rock. Developments in Geotechnical Engineering, 76. Elsevier Publ. Co (ISBN: 0:444-89449-7).

[14] Pusch, R., Karnland, O., Lajudie, A. and Decarreau, A. (1993). MX-80 exposed to high temperatures and gamma radiation. SKB Technical Report TR-93-03. SKB, Stockholm.

[15] Pusch, R. and Madsen, F.T.(1995). Aspects of the illitization of the Kinnekulle bentonites, 1993. Clays and Clay Minerals, 43,3:133-140.

[16] Pusch, R., and Yong, R.N. (2006). Microstructure of smectite clays and engineering performance. Taylor & Francis Group, New York.

[17] Pusch, R. (2008). Geological storage of radioactive waste. Springer-Verlag, Berlin, Heidelberg. ISBN: 978-3-540-77332-0.
[18] Pusch, R., Yong, R.N. and Nakano, M. (2010). Stiffening of smectite buffer clay by hydrothermal effects. Eng. Geol. Vol. 116, pp.21-31.
[19] Pusch, R., Ramqvist, G., Kasbohm, J., Knutsson, S. and Mohammed, M.H. (2012). The concept of highly radioactive waste (HLW) disposal in very deep boreholes in a new perspective. Journal of Earth Sciences and Geotechnical. Engineering, Vol.2, No.3, pp.1-24.
[20] Pusch, R., Warr, L., Grathoff, G., Pourbakhtiar, A., Knutsson, S. and Mohammed, M. H. (2013). A talc-based cement-poor concrete for sealing boreholes in rock, 2013. Engineering Geology, Vol.5, pp.251-267.
[21] Pusch, R. (2015). Bentonite Clay. CRC Press (Taylor and Francis), USA.
[22] Pusch, R., Yong, R.N. and Nakano, M. (2018). Geologic disposal of high-level radioactive waste. Taylor & Francis, N.Y.
[23] Yang, T. Weston, R. and Pusch, R. (2019). Time-dependent physical interaction of clay and rock in hlw repositories. Journal of Earth Sciences and Geotechnical. Engineering, Vol.9, No.3, pp.275-295.
[24] Xiaodong, L., Prikryl R. and Pusch, R. (2011). THMC-testing of three expandable clays of potential use in HLW repositories. Appl. Clay Science, 52, pp.419-42).
[25] Yang, T., Pusch, R., Knutsson, S. and Xiaodong, L.(2015). Lab testing of method for clay isolation of spent reactor fuel in very deep boreholes. Proc. Earth and Planetary Science, 15, pp.152-158.